Parkinson's Disease

36

Martin Niethammer and Ana M. Franceschi

Parkinson's Disease

Parkinson's Disease (PD) is a chronic progressive movement disorder characterized by a combination of clinical features, including resting tremor, rigidity, bradykinesia, gait disturbance, and postural instability [1, 2]. PD is rare before age 50, with the incidence rising with age [3]. The mean age of onset is 60 years, and men are 1.5–2 times more likely than women to develop PD, although this gender ratio has not been seen in all populations [4, 5]. Earlier-onset PD progresses at a slower rate and is associated with more levodopa-induced complications [2]. While the majority of PD remains idiopathic, a number of genetic risk factors have been identified as causative of PD. In particular, G2019S mutation in the leucine-rich repeat kinase 2 (LRRK2) gene and several variations in the glucocerebrosidase (GBA) gene are frequent in some populations, including Ashkenazi Jewish, where they may account for up to one third of sporadic PD [6–8].

The pathological hallmark of PD is selective loss of pigmented dopaminergic neurons in the pars compacta of the substantia nigra coupled with widespread deposition of Lewy bodies (aggregates of alpha-synuclein) in the brainstem, spinal cord, and cortex [9–11]. While the definitive diagnosis of PD requires pathological confirmation, clinically PD is defined by its motor symptoms. Onset is typically unilateral, with asymmetry persisting throughout the disease course. Subtle changes, often having been present preceding the diagnosis, include reduced facial expression, a lack of arm swing, monotonous speech, loss of gesturing during talking, a lack of coordination, and a change in handwriting. Current diagnostic criteria require the presence of bradykinesia with at least on other cardinal motor features such as tremor or rigidity, in addition to a number of supporting and exclusionary criteria [12, 13]. It is increasingly recognized that PD is also characterized by a number of non-motor clinical manifestations, including mood disturbances, cognitive dysfunction, constipation, and sleep disorders, many of which may be present for years preceding the motor symptoms. Indeed, REM sleep behavior disorder (RBD) is now seen as one of the biggest nongenetic risk factors for the development of PD [14]. While PD is the most common form of degenerative parkinsonism, atypical parkinsonian syndromes (APS), specific syndromes with distinct symptomatology, pathologies, and prognosis, represent as much as 15–20% of parkinsonism seen in specialty practices. These include other disorders of dopaminergic dysfunction such as multiple system atrophy (MSA), progressive supranuclear palsy (PSP), and corticobasal degeneration (CBD) [15]. Diagnostic accuracy (established with postmortem brain examination) approaches well over 95% in movement disorder specialty practices when patients are followed over time, with much lower accuracy early in the disease or with APS [12, 16]. Neuroimaging has not yet been included in the diagnostic criteria of PD or any of the APS, though several modalities can be helpful in that regard and will be discussed in detail below.

Structural Imaging

Magnetic Resonance Imaging

Conventional MRI shows mostly nonspecific findings in PD, but in clinical practice it is essential to differentiate neurodegenerative from symptomatic parkinsonism as it allows us to exclude underlying pathologies such as inflammatory diseases, brain tumors, normal-pressure hydrocephalus, vascu-

M. Niethammer
Donald and Barbara Zucker School of Medicine at Hofstra/Northwell, The Feinstein Institutes for Medical Research, Manhasset, NY, USA

Department of Neurology, North Shore University Hospital, Manhasset, NY, USA

A. M. Franceschi (✉)
Donald and Barbara Zucker School of Medicine at Hofstra/Northwell, The Feinstein Institutes for Medical Research, Manhasset, NY, USA

A. M. Franceschi, D. Franceschi (eds.), *Hybrid PET/MR Neuroimaging*, https://doi.org/10.1007/978-3-030-82367-2_36

lar disorders, Wilson's disease, bilateral striatopallidodentate calcinosis, manganese-induced parkinsonism, and different subtypes of neurodegeneration associated with brain iron accumulation [17–19].

In recent years, several groups described an MRI finding that has the potential to distinguish PD from healthy controls. On iron-sensitive MRI sequences at high field strength (3 or 7 Tesla), PD subjects lack a hyperintense area within the dorsolateral border of the hypointense substantia nigra pars compacta [20–22]. In healthy controls the presence of this dorsolateral nigral hyperintensity (DNH) is commonly referred to as the "swallowtail sign," and its loss is thought to reflect nigral pathology. Meta-analysis suggests that the absence of DNH has a high sensitivity and specificity to distinguish PD from healthy controls (combined 3 T and 7 T imaging) [23]. Including patients with other forms of parkinsonism, DNH was also found to be absent in 89.4% of atypical parkinsonian disorders compared to 21.4% of nondegenerative parkinsonism, including drug-induced parkinsonism [23, 24]. Similarly, in dementia patients, the absence of DNH may be useful in distinguishing dementia with Lewy bodies from frontotemporal dementia or Alzheimer's disease [25]. One study found that the concordance rate between loss of DNH and abnormal presynaptic dopaminergic imaging is 86%, suggesting that high field strength MRI might be usable in the clinical setting instead of nuclear medicine imaging [26].

MRI also can play a role in discriminating idiopathic PD from atypical Parkinsonian disorders, though the sensitivity is low early in the disease course. T1-weighted sequences are important for anatomical detail and provide good gray matter/white matter contrast. By using an inversion pulse, the contrast of T1-weighted images can be improved as in the MP-RAGE (magnetization-prepared rapid acquisition with gradient echo) sequence which results in high-resolution 3D datasets. The use of a ratio of images acquired by two distinct inversion recovery sequences, depending only on T1, one designed to suppress the white matter and the other to suppress the gray matter, when combined is sensitive to cell loss and reveal structural changes in the substantia nigra in PD patients. The inversion recovery techniques reveal decreased ratio between the substantia nigra and midbrain area, with the most affected lateral and caudal substantia nigra in PD and the opposite in PSP [17], correlating with the pathophysiology of idiopathic PD [27].

In MSA, atrophy of the putamen, midbrain, cerebellum, and corpus callosum as well as the "hot cross bun" sign and a hyperintense putaminal rim can be seen on structural MRI sequences [28, 29], while the characteristic findings in PSP are the "humming bird" and "morning glory signs" relating to midbrain atrophy [30]. Reduced midbrain/pons ratio separates PSP from PD, while lower middle cerebellar/superior cerebellar peduncle ratio may be characteristic of MSA [31]. These findings vary in their utility. The humming bird sign has a high specificity for PSP [30], while about 55% of patients with the "hot cross bun" sign have a disease other than MSA [32, 33]. Moreover, they are rarely present in the first few years of the disease, when the clinical need for accurate diagnostics is greatest.

Transcranial Sonography

Transcranial sonography (TCS) depicts the substantia nigra through an acoustic temporal bone window as an area of hyperechogenicity in the midbrain and is found in up to 95% of patients with PD patients, hypothetically reflecting vulnerable nigral dopamine neurons and increased iron content [34–38]. In contrast, in normal controls, such hyperechogenicity is only found in about 3–13% of subjects. This hyperechogenicity is observed in very early stages of the disease and generally remains unchanged with advancing stages of PD [37], though in at least one study, it was found to correlate with disease duration in males (but not females) [39]. While the finding has high sensitivity and specificity constituting a potential biomarker for PD in early stages, it therefore cannot be used to monitor disease progression [40, 41]. In addition, TCS findings in PS include hyperechogenicity of the lenticular nucleus (11–25% of subjects) and caudate nucleus (50–75%), as well as hypoechogenicity in the midbrain Raphe (25–30%) [42].

An increase in total iron content in the substantia nigra also occurs in MSA and PSP, but in these entities it has been suggested that iron is bound by increased amounts of ferritin whereas in idiopathic PD ferritin is decreased. Thus, in PD the increased amounts of iron must have alternative binding proteins considered to contribute to the degeneration of the substantia nigra and leading to hyperechogenicity [42]. Nevertheless, hyperechogenicity of SN may also be seen in corticobasal degeneration, Wilson's disease, essential tremor, depression, and spinocerebellar ataxia type 3. To some degree, SN hyperechogenicity alone can differentiate between PD and MSA-P [43]. Combining the different TCS findings increases accuracy – substantia nigra hyperechogenicity associated with normal echogenicity of the basal ganglia has a positive predictive value of 0.91 for idiopathic PD whereas the combination of normal echogenicity of the substantia nigra and hyperechogenicity of the lenticular nucleus has a high predictive value for MSA-P and PSP [35, 37, 42].

Additional increases in sensitivity and specificity in the differentiation of PD from APS can be obtained by combining TCS findings with clinical features such as hyposmia, myocardial scintigraphy, or motor asymmetry. Izawa et al. reported olfactory dysfunction in 80–90% of patients with PD. When associated with substantia nigra hyperechogenicity, it improves diagnostic sensitivity for PD diagnosis to near 100% [34]. Likewise, the combination of SN hyper-

echogenicity, hyposmia, and motor asymmetry yields sensitivity, specificity, and PPV of 49%, 98%, and 97%, respectively, in the differentiation of PD from other parkinsonism [44]. TCS may also be useful in following preclinical PD [14, 45]. In a 10-year prospective population-based study, the relative risk for developing PD was 7.43, 3.60, and 5.52 for baseline SN hyperechogenicity, hyposmia, and mild parkinsonian signs, respectively [46].

The main advantages of TCS are wide availability, repeatability, safety, real-time imaging, noninvasiveness, and cost-effectiveness, but optimal transcranial US results depend on a sufficient temporal bone acoustic window, quality of the US system, post-processing technology, and on the experience of the investigator. In some populations, the percentage of subjects with insufficient temporal windows may be as high as 60% [38], and to date TCS has not entered routine clinical practice.

Functional Imaging

Positron emission tomography (PET) and single-photon emission computed tomography (SPECT) imaging use radiotracers for in vivo assessment of normal and abnormal brain function. These techniques have been extensively used to study the dopaminergic system in parkinsonian disorders, but other neurochemical systems have also been investigated, and cerebral blood flow or glucose utilization can be mapped with radiolabeled water and glucose [47]. In general, SPECT imaging is less expensive and more widely available than PET imaging. As such, routine SPECT can be performed in most nuclear medicine departments without the need for an on-site cyclotron. However, PET has superior spatial resolution and higher sensitivity than SPECT. In regard to parkinsonian disorders, the resolution in SPECT limits the separation of caudate and putamen, while the higher sensitivity of PET allows for shorter imaging times.

Dopaminergic Imaging

Presynaptic Dopaminergic Imaging

Motor symptoms in patients with PD correlate with degeneration of dopaminergic neurons in the SN and subsequent loss of their projections to the striatum. The presynaptic function of these nigrostriatal projections can be assessed with the use of various radiolabeled tracers. 6-[^{18}F]Fluoro-L-dopa (FDOPA) PET is considered the gold standard in the assessment of dopaminergic neurons in the striatum [48]. The level of FDOPA uptake corresponds to the level of radiotracer uptake into the presynaptic terminal, dopa-decarboxylase (AADC – aromatic amino acid decarboxylase) activity, and vesicular storage in the presynaptic dopaminergic neurons [49]. The characteristic findings include asymmetric reduction of FDOPA uptake in PD patients, with greater reductions contralateral to the clinically more affected side. Radiotracer binding is lowest in the contralateral putamen as compared to the caudate nucleus, referred to as the rostro-caudal gradient of FDOPA uptake [50]. In early disease, there is a relative increase in FDOPA uptake as compared to VMAT2 (vesicle monoamine transporter 2).

[^{11}C]-Dihydrotetrabenazine (DTBZ) PET is a marker of vesicle monoamine transporter 2 (VMAT2) activity, which is found predominantly in the nerve terminals of the dopaminergic projections in the striatum. The level of DTBZ binding corresponds to the amount of dopamine uptake into intraneuronal vesicles at the presynaptic nerve terminal [49]. Furthermore, protocols of up to 4 hours also allow for assessment of dopamine turnover by measuring changes in its inverse, the effective dopamine distribution volume (EDV) [51, 52]. These studies demonstrate compensatory increases in dopamine turnover when compared to reductions in dopamine synthesis and storage measured, indicating that EDV may serve as a more sensitive marker of early PD. Unlike FDOPA and DAT imaging in PD, there is no compensatory change in the level of DTBZ activity associated with degeneration of dopaminergic nerve terminals and disease progression [53], and therefore, VMAT2 expression may be the best reflection of the actual level of denervation in the affected striatum. It is, however, affected by treatment, as there is a reduction in striatal DTBZ binding following L-DOPA challenge in patients with advanced PD, likely reflecting increased vesicular DA levels [54].

Dopamine transporter (DaT) activity is assessed via various PET and SPECT tropane (cocaine-derived) radiotracers ([^{123}I]-beta-CIT, [^{123}I]-FP-CIT, [^{18}F]-FP-CIT, [^{18}F]-CFT, [^{11}C]-CFT, [^{11}C]-RTI-32, [^{11}C]-WIN35,428, [^{11}C]-PE2I-BP [55–60]) and non-tropane analogs ([^{11}C]-nomifensine, [^{11}C]-methylphenidate [49, 61]) (Fig. 36.1). Since the DA transporter is involved in the reuptake of dopamine from the synaptic cleft, the level of DAT activity directly corresponds to the number of presynaptic dopaminergic nerve terminals in the striatum. SPECT imaging with [^{123}I]-FP-CIT (DaT scan) is currently FDA approved for the differentiation of PD from essential tremor. While such presynaptic imaging in general cannot distinguish between PD and APS, it is helpful in separating dopaminergic degeneration from nondegenerative parkinsonism, such as vascular or drug-induced parkinsonism [62–64]. Some studies have suggested that early-phase [^{18}F]-FP-CIT PET images, which contain information related to perfusion [65], may be able to differentiate PD from MSA or PSP, but this approach has not been validated in prospective studies [66, 67].

Reductions in FDOPA-PET uptake have consistently shown to best correlate with disease severity and clinical bradykinesia scores, while the correlation with rigidity and

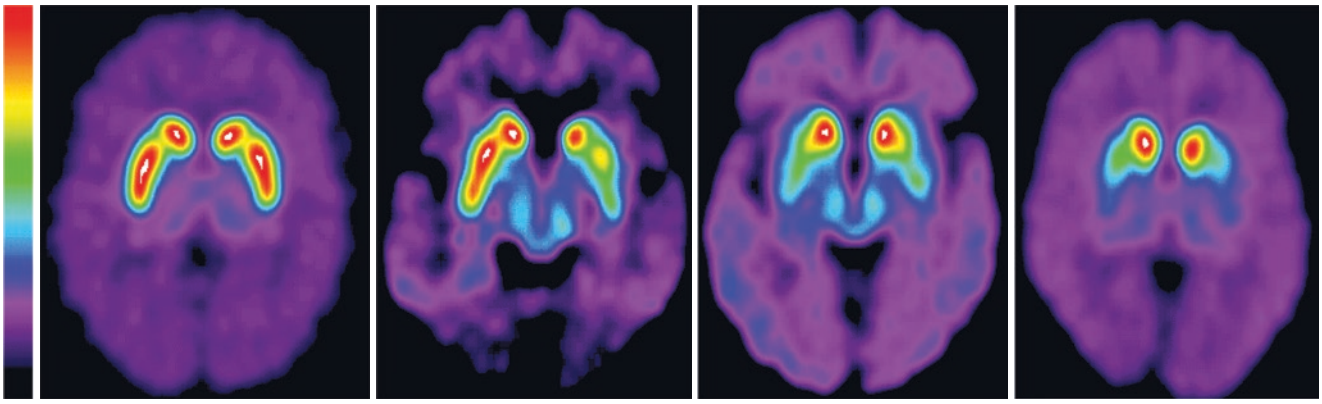

Fig. 36.1 FP-CIT Staging of disease severity. [^{18}F]-FP-CIT uptake is delineated from the background activity in the brain. *Normal:* In normal subjects, uptake is bilaterally symmetrical and of uniform thickness in both caudate and putamen (crescent shapes). *Stage 1, mild:* [^{18}F]-FP-CIT uptake is asymmetric in the putamen; near normal on one side but reduced on the contralateral side with respect to the background, especially in the posterior part. Caudate uptake is relatively preserved on both sides and clearly delineated from the background. *Stage 2, moderate:* [^{18}F]-FP-CIT uptake is bilaterally reduced with respect to the background in the putamen but still relatively preserved in the caudate nuclei. *Stage 3, severe:* [^{18}F]-FP-CIT uptake is bilaterally reduced significantly with respect to the background in the putamen and somewhat reduced in the caudate nuclei. (Images courtesy of D. Eidelberg, MD)

postural disturbance is less significant [68, 69], while there is no correlation between tremor and the level of dopaminergic deficit, pointing towards the involvement of other neural circuits in the pathogenesis of Parkinsonian tremor [69]. Due to compensatory downregulation of DaT activity in early PD secondary to the denervation of dopaminergic neurons, DaT scans tend to overestimate the percentage of remaining nigrostriatal projections as compared to VMAT2 or FDOPA imaging [49]. Nevertheless, like FDOPA imaging, DaT studies demonstrate a significant correlation between radiotracer uptake and the severity of clinical disease as measured by the Hoehn and Yahr scale and Unified Parkinson Disease Rating Scale (UPDRS) [56].

Dopaminergic tracer uptake declines with disease progression. In an FDOPA-PET study of de novo PD patients, mean presynaptic dopaminergic function at the time of the first PET scan varies from 45% in the posterior putamen to 76% of the control mean in the caudate nucleus [70]. If it is assumed that the loss of radiotracer binding is a linear function, extrapolating back from these values allows for the calculation of the pre-symptomatic period, which is estimated to be 6.5 years for the posterior putamen [70, 71]. Following disease onset, the yearly rate of DA loss is greatest in the putamen, ranging from 4 to 13% according to FDOPA imaging studies, although the absolute decline is equal in the entire striatum [70, 71]. Similarly, DaT PET imaging with [^{18}F]-CFT PET calculated annual decline in radiotracer uptake to be 13.12% of the baseline mean in the putamen and 12.5% of the baseline mean in the caudate nucleus, with no significant correlation between the change in [18F]-CFT uptake and Unified Parkinson's Disease Rating Scale (UPDRS) scores [72]. Similarly, the annual decline in striatal uptake assessed by DaT SPECT ([^{123}I]-beta-CIT) was calculated to be 11.2%/year from the baseline scan, compared with 0.8%/year in controls.

This decline precedes symptom onset. Patients with hemiparkinsonism (i.e., with no symptoms yet on one side of their body) already exhibit reduced tracer uptake in the bilateral striatum, including ipsilateral to the clinically affected side, indicating preclinical disease [71, 73, 74]. Moreover, in subjects with REM sleep behavior disorder (RBD), which is considered a strong risk factor for the development of synucleinopathy, tracer uptake in the putamen progressively decreases from controls to idiopathic RBD and PD patients with RBD, while tracer uptake in the caudate nucleus overlaps between patients with idiopathic RBD and those with PD without RBD [75].

Again, while there was a significant correlation between [^{123}I]-beta-CIT binding and disease severity quantified by UPDRS, there was no association between the annual rate of disease progression and change in clinical scores [76]. Furthermore, the progression of imaging findings correlated only with age and degree of dopaminergic loss at symptom onset, with slower progression in younger-onset patients and those with a greater reduction in tracer binding at baseline [76]. Likewise, studies looking at the efficacy of dopaminergic therapy in PD have repeatedly demonstrated a poor correlation between the progression of clinical symptoms and functional imaging findings [15, 77]. Similarly, trials looking at novel treatment options, such as human embryonic mesencephalic tissue grafts, have consistently shown increased FDOPA binding in the grafted putamen, indicating graft sur-

vival [78–80], which do not necessarily correlate with improvement in clinical symptomatology [81, 82].

Normal Dopaminergic Imaging in PD

Several clinical studies have noted normal dopaminergic imaging in 10–15% of subjects with a clinical diagnosis of PD, which were termed "SWEDDs" – scans without evidence of dopaminergic deficit [15, 77, 83]. While this raised concern that dopaminergic imaging thus might miss patients with PD, follow-up diagnoses in 150 patients with normal DaT imaging at baseline revealed that 97% were reclassified to nondegenerative parkinsonism (vascular Parkinsonism, drug-induced Parkinsonism) or tremor (dystonic tremor, essential tremor), indicating that normal DaT imaging supports the diagnosis of movement disorders other than PD in the majority of cases [84]. Likewise, in the PRECEPT study, 91/799 subjects were classified as SWEDD at baseline. A total of 72 subjects had repeat imaging at 22 months, and 66/72 remained as SWEDD. In contrast 626/629 subjects with abnormal DaT scans at baseline remained abnormal at follow-up. The clinical diagnosis was changed in 44% of SWEDD subjects over the course of the study [85]. This was further confirmed with an FDG PET study looking at SWEDD patients, which revealed low Parkinson-related metabolic patterns and a lack of clinical progression in these subjects [86]. Prospective trials have found increased agreement between initial dopaminergic imaging results and diagnosis based on clinical assessment at a later time point, therefore suggesting that patients with normal dopaminergic imaging are unlikely to have idiopathic PD [87, 88].

Postsynaptic Dopaminergic Imaging

Striatal output in the basal ganglia is facilitated by both D1 and D2 receptors. D1 receptor activity, assessed using [^{11}C]-SCH-23390 [89] and [^{11}C]-NNC- 112 [90], is normal in PD with a symmetric distribution of radiotracer uptake between the hemispheres, in contrast to other neurodegenerative disorders characterized by loss of striatal neurons such as MSA [89]. Evaluation of D2 receptor function may be done utilizing antagonistic radiotracers such as [^{123}I]-epidepride [91] and [^{123}I]-(S-)-2-hydroxy-3-iodo-6--methoxy-N[(1-ethyl-2-pyrrolidinyl) methyl]-benzamide ([^{123}I]-IBZM) [92] for SPECT or [^{11}C]-raclopride [93] and [^{18}F]-desmethoxyfallypride [94] for PET imaging, which have a greater affinity for the receptor when compared to D2 agonists. In early PD, [^{11}C]-raclopride PET has repeatedly demonstrated increased receptor binding in the putamen contralateral to the clinically affected side, likely secondary to compensatory upregulation of D2 receptors on the postsynaptic nerve terminals in response to decreased dopamine levels [93–95]. On the other hand, patients with advanced disease demonstrate reduced [^{11}C]-raclopride uptake in the entire striatum, which tends to be more prominent in the caudate nucleus as compared to the ipsilateral putamen [95, 96].

These changes in the density of postsynaptic D2 receptors in patients with PD may be secondary to chronic L-DOPA therapy or occur independently of treatment [95]. Studies have postulated that this decrease in the number of postsynaptic receptors is likely induced by chronic dopaminergic therapy rather than disease progression [96]. In addition, various interventions, such as D-amphetamine [97, 98], placebo administration [99], L-DOPA therapy [100, 101], repetitive transcranial magnetic stimulation (rTMS) [102], and neural transplantation of embryonic mesencephalic tissue [79, 100], have all resulted in decreased [^{11}C]-raclopride PET and [^{123}I]-IBZM SPECT uptake in the affected striatum. Since these changes in radiotracer uptake correlate with increased levels of endogenous dopamine in the synaptic clefts, D2 receptor imaging can serve as a biomarker of therapeutic intervention in patients with PD.

Reductions in [^{11}C]-raclopride uptake following L-DOPA challenge in the striatum of PD patients signify increased levels of endogenous dopamine binding to the postsynaptic D2 receptors in response to dopaminergic therapy. These changes in tracer binding were associated with significant improvement in bradykinesia and rigidity, but not in tremor as assessed by the UPDRS [103].

Postsynaptic imaging has helped to give some insight into motor complications of chronic levodopa therapy, including fluctuation and peak-dose dyskinesias. Using [11C]-raclopride PET, de la Fuente-Fernandez and colleagues found that in patients with motor fluctuations, synaptic dopamine levels were three times higher than in those without fluctuations, and advance PD patients lose their ability to regulate synaptic dopamine release [104, 105]. This dysregulation also may relate to the development of dyskinesias, as larger changes in raclopride binding relate to higher dyskinesias score [103, 106]. It should be noted that this likely is not the only mechanism involved in the development of dyskinesias, as recent studies have also implicated changes in the cerebral vasomotor response to levodopa [107–109]. Another complication of dopaminergic therapy is the development of impulse control disorders and dopamine dysregulation syndrome. Several raclopride studies have shown that these disorders are not related to changes in dopamine levels in the dorsal striatum but rather the ventral striatum, similar to drug addiction [110–112].

While presynaptic dopaminergic imaging is of little utility in the differentiation of PD and APS, postsynaptic imaging does show some promise. In contrast to upregulated tracer binding in the striatum of early PD [94, 113], striatal D2 binding has been found to be markedly reduced in MSA and PSP [114, 115] while relatively preserved in CBD [116, 117]. Nonetheless, the role of [^{123}I]-IBZM SPECT on the dif-

ferential diagnosis of parkinsonism remains controversial. In a [^{123}I]-IBZM SPECT study, Vlaar et al. reported a low accuracy in differentiating between PD and APS [118], while another SPECT study suggests that a combination of [^{123}I]-FP-CIT, [^{123}I]-IBZM, and meta-[^{123}I]-iodobenzylguanidine (MIBG) scintigraphy resulted in high accuracy of 94% sensitivity and 94% specificity in differentiating PD from APS [119]. More studies are needed to investigate the utility of these imaging tracers in the diagnosis of atypical parkinsonian syndromes.

Metabolic Imaging

Functional imaging with [^{18}F]-fluorodeoxyglucose (FDG) PET measures glucose utilization of neurons, providing an estimate of rest-state regional and global metabolism in the brain. This technique has been used extensively in parkinsonian disorders to identify disease-specific changes in neural activity [120]. A number of analytical approaches have been used to identify abnormal brain networks in normal aging and neurological disease [121–124], as outlined below.

The PD-Related Motor Pattern

In PD, [^{18}F]-FDG PET imaging reveals hypermetabolism in the globus pallidus, putamen, thalamus, pons and cerebellum, and hypometabolism in the frontal and parietal association areas [125, 126]. However, in order to develop biomarkers that can quantify network expression in individual subjects, multivariate approaches are needed [127] and have been widely used in defining and studying abnormal networks in neurodegenerative disorders such as PD, APS, AD, FTD, and Huntington's disease [128–134]. One such method, spatial covariance analysis, detects network-level functional abnormalities in a variety of neurodegenerative disorders, including PD (Eidelberg et al. 1994; Eckert et al.2007b), APS, HD, and dementia [135–139]. The details of this method based on principal component analysis (PCA) have been reviewed elsewhere [140, 141]. Briefly, the scaled subprofile model (SSM) is applied to metabolic imaging data in a combined sample of scans from healthy subjects and patients. Once a pattern is identified that distinguishes one group from the other, its expression can then be prospectively quantified on an individual basis, and the resulting subject scores can be correlated with clinical and physiological measures of interest, aid in the diagnosis, or followed with disease progression.

The most validated network pattern is the Parkinson's disease-related pattern (PDRP), which is characterized by increased pallidothalamic and pontine metabolic activity and relative reductions in the premotor cortex, supplemental motor area, and parietal association regions [130]. Abnormally elevated PDRP expression does not simply discriminate patients with PD from healthy subjects, but also can distinguish between PD and APS (described below). The PDRP topography has been identified in a number of independent patient populations regardless of medication state of scanner parameters [142–150] (Fig. 36.2). PDRP was identified primarily in subjects on dopaminergic therapy; however, a very similar abnormal network can be identified in PD subjects who have never been on therapy [151]. Subject scores (which denote pattern expression levels in individual patients) show excellent within-subject reproducibility on repeat scanning [152]. Furthermore, since metabolism and cerebral blood flow are coupled, at least in the absence of dopaminergic medication [153], PDRP expression can also be measured in scans of resting cerebral perfusion obtained with [^{15}O]-H2O PET [154] or 99mTc-ethylcysteinate dimer (ECD) SPECT [155], though larger studies with these modalities are lacking.

PDRP expression correlates strongly with spontaneous subthalamic nucleus activity recorded intraoperatively during deep brain stimulation surgery, linking abnormal PDRP functional topography directly to alterations of basal ganglia pathways [156]. Some studies have found metabolic correlations with striatal and frontal FDOPA uptake [157, 158], while a more recent study found even more widespread correlations between FDOPA uptake and PDRP-related areas [145].

Individual PDRP expression scores consistently correlate with Unified Parkinson's Disease Rating Scale (UPDRS) motor ratings of bradykinesia and rigidity [130, 149, 159–162], while tremor shows a relation with a distinct tremor-related pattern. Additionally, PDRP expression normalizes with treatment, either with dopaminergic medication or deep brain stimulation, though it remains elevated relative to healthy controls [149, 163, 164].

Metabolic Imaging and Preclinical PD

Similar to dopaminergic imaging, PDRP expression is already abnormal prior to the onset of symptoms. In patients with hemi-parkinsonism, PDDR expression is similarly elevated in both brain hemispheres at baseline, with parallel and fairly linear increases on follow-up scans [71, 165], suggesting that PDRP does not simply reflect symptoms. Indeed, PDRP expression may be able to serve as a biomarker in the prodromal stages of the disease.

The presence of REM sleep behavior disorder (RBD) appears to confer an especially high risk of PD [14]. Patients with idiopathic RBD (iRBD) have reduced uptake on dopaminergic imaging [75], and up to 50% of patients with iRBD develop a synucleinopathy within 5 years (most often PD but also dementia with Lewy bodies (DLB) or MSA) [166]. Voxel-wise comparison between iRBD subjects and healthy controls has found increased metabolism in the hippocampus/parahippocampus, cingulate gyrus, supplementary

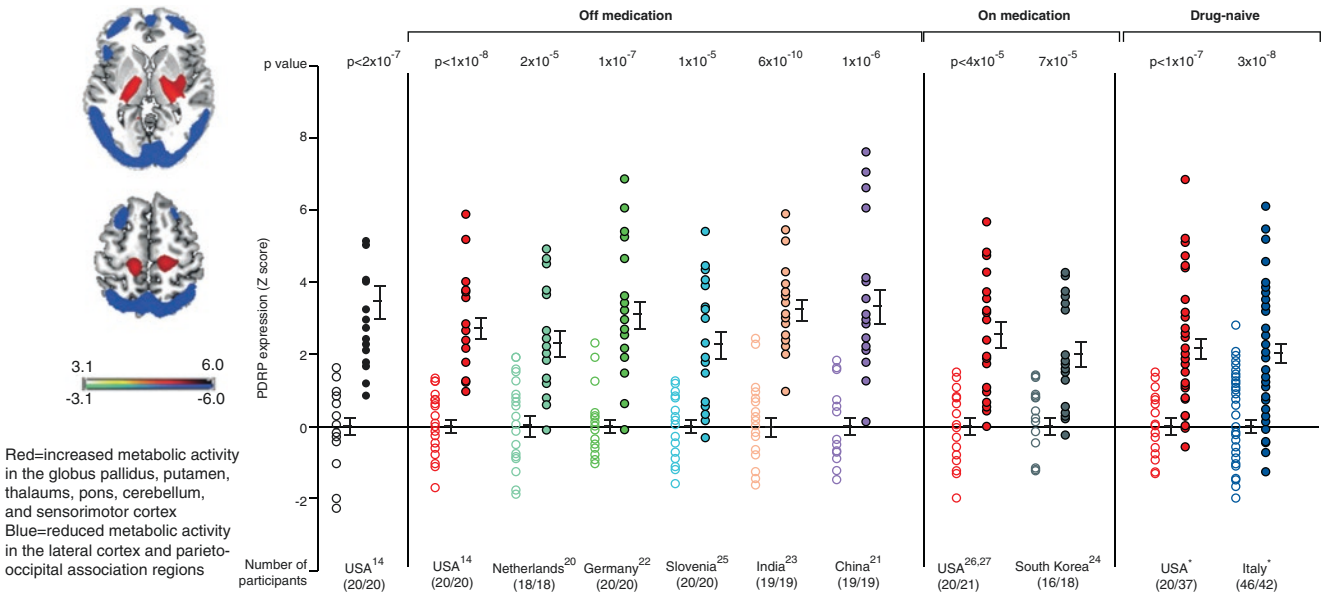

Fig. 36.2 Discovery and validation of the Parkinson's disease-related pattern. (**a**) The Parkinson's disease-related pattern (PDRP) displayed as voxel weights (i.e., regional loadings) thresholded at Z = 3.1 ($p < 0.001$) and overlaid on T1-weighted MRI template. (**b**) Data are Z scored with respect to healthy control values; means (SE) are presented to the right of the individual data. PDRP expression was increased in patients with Parkinson's disease (closed circles) relative to healthy controls (open circles) in the North Shore University Hospital derivation cohort ($p < 2 \times 10^{-7}$), and it was consistently elevated across six independent testing samples when scanned in a medication-free (OFF) state. Significant PDRP elevations were also observed in Parkinson's disease cohorts who were scanned in a medicated (ON) state (USA, South Korea) and in two cohorts of newly diagnosed patients who had not yet begun drug therapy (denoted by *: USA, courtesy of Chris C Tang, The Feinstein Institute for Medical Research, Manhasset, NY, USA; Italy, courtesy of Flavio M Nobili, University of Genoa, Genoa, Italy). These results show that the underlying pathogenic changes are quantifiable regardless of the patients' disease stage or treatment state. Slight differences in mean PDRP expression scores across the different cohorts are due to group differences in disease duration and severity. (Reprinted from Schindlbeck and Eidelberg [150], with permission from Elsevier)

motor area, and pons and decreased metabolism in the occipital/lingual gyrus; metabolism in several of these areas correlated either with disease duration or chin electromyography [167]. On a network level, PDRP expression has been studied in at least four independent cross-sectional iRBD cohorts. In each case, PDRP expression was found to be elevated compared to healthy controls, in general at intermediate levels between PD and healthy controls [168–171]. On long-term follow-up, iRBD patients that convert to PD or DLB have elevated PDRP expression at baseline, while abnormally low PDRP scores (in the negative range) seem to favor conversion to MSA [168]. Separate metabolic covariance patterns for iRBD were recently described in two cohorts with topographies that show partial overlap with PDRP [169, 171]. Expression of one of these iRBD-related patterns was similar in PD patients regardless of the presence of RBD, suggesting a possible common pathway. Indeed, expression of both PDRP and iRBDRP was higher in patients with a more severe form of PD, suggesting that iRBDRP is an early manifestation of PDRP [171].

The PD-Related Tremor Pattern

Tremor in PD is somewhat distinct, as it does not consistently respond to dopaminergic treatment and its pathophysiology is thought to involve cerebellothalamocortical pathways in addition to the cortico-striato-pallido-thalamocortical motor circuits that lead to bradykinesia and rigidity [172]. Accordingly, PDRP expression is not affected by the severity or presence of parkinsonian tremor [160, 173, 174].

OrT/CVA is an algorithm that relies on supervised principal component analysis (PCA) to identify distinct spatial covariance patterns with consistent changes in subject expression across experimental conditions [175]. Applying OrT/CVA to [^{18}F]-FDG PET images from PD patients with tremor acquired at baseline and after tremor suppression with deep brain stimulation, Mure et al. identified a network that specifically relates to PD tremor [176]. This tremor-related pattern, termed PDTP, is characterized by hypermetabolism in the cerebellum/dentate nucleus and primary motor cortex and, to a lesser degree, caudate/putamen, brain regions known to be connected through the Vim thalamic nucleus [177, 178]. At baseline, without stimulation, PDTP scores correlated significantly with concurrent measurements of tremor amplitude, while Vim stimulation resulted in consistent reductions in pattern expression along with clinical improvement.

Conversely to PDRP (which is correlated with akinesia and rigidity), prospective PDTP computations in an indepen-

dent group of 41 PD patients showed this network to be related to the severity of tremor, but not akinesia-rigidity, highlighting the functional difference between these two PD-related metabolic networks [176]. Comparison of the effects of Vim thalamic and subthalamic nucleus stimulation on network activity during tremor suppression further underscored these differences. At baseline, PDTP expression was abnormally elevated in PD patients with either Vim thalamic or subthalamic nucleus (STN) DBS implanted electrodes. In line with clinical experience, tremor was improved by stimulation at either target, whereas only STN stimulation improved akinesia-rigidity. Accordingly, both stimulations led to reductions of abnormally elevated PDTP scores. On the other hand, baseline PDRP elevations were only suppressed by STN DBS, consistent with clinical benefit [176]. Thus, PDTP and PDRP appear to be functionally independent networks, both as symptom biomarkers and targets of intervention.

The PD Cognition-Related Pattern

In addition to the motor signs and symptoms of Parkinson's disease, non-motor symptoms can be prominent and even precede motor symptoms [14, 179]. Cognitive dysfunction can be substantial in PD, typically appearing later in the disease and progressing slower [180].

The nature of progression to cognitive impairment in PD is not entirely clear, but likely involves multiple transmitter systems, beginning with dopaminergic dysfunction, but also cholinergic or noradrenergic systems later on in the disease [181–185]. Cortical metabolic reductions are often evident early in PD, even in cognitively intact patients [138, 186, 187]. Moreover, different neuropsychiatric symptoms correlate with distinct metabolic changes in PD, such as cognitive dysfunction with posterior cingulate and temporoparietal lobe hypometabolism and depressive symptoms with amygdala hypermetabolism [162, 188–190]. Spatial covariance analysis has revealed a specific metabolic topography associated with cognitive function in PD, termed PDCP. PDCP is characterized by hypometabolism in the dorsolateral prefrontal cortex, rostral supplementary cortex, precuneus, and posterior parietal regions, in association with relative metabolic increases in the cerebellum [138, 191, 192]. Similar to PDRP, PDCP is not restricted to a single imaging site or scanner, as a comparable pattern has been derived independently from a separate cohort imaged with a different scanner, with af high correlation between expression scores of the two versions [193].

Clinically, PDCP expression correlates with performance on neuropsychological tests of memory and executive functioning (but not motor disability) in the original cohort, as well as independent validation cohorts [191, 193]. Although originally identified in a cohort of non-demented PD patients, PDCP expression increases with increasing cognitive dysfunction, with substantial increases seen in PD patients with dementia or in DLB [147, 194]. The PDCP topography involves both dopaminergic and cholinergic afferents to the cerebral cortex, and abnormal network expression is similar in patients with PD dementia and DLB. There is relative sparing of the medial temporal lobes in PDD compared to AD, and accordingly, PDCP topography is distinct from that of an independently derived AD-related pattern [194, 195].

Functionally, the two main PD-related metabolic patterns (PDRP and PDCP) are independent. Although both PDRP and PDCP expression progress over time, PDCP expression lags behind [71, 150], consistent with cognitive dysfunction typically developing later in the course of PD. PDRP expression correlates with dopaminergic dysfunction in the caudate and putamen, though this remains significant only in the posterior putamen once corrected for PDCP [145]. Conversely, PDCP expression is correlated with dopaminergic dysfunction in the anterior striatum [145, 196], highlighting the importance of caudate circuitry for cognitive functioning. However, the correlations between PDCP expression and striatal dopaminergic function are modest, and PDCP activity is not simply determined by dopaminergic dysfunction in the caudate, but extrastriatal dopaminergic and other neurotransmitter systems are likely to be involved as well.

MRI Equivalents of PD-Related Networks

While PD-related covariance patterns have been well characterized and validated in [^{18}F]-FDG PET scans, this approach relies on the use of radiotracers (exposing subjects to radiation) and availability, as the technology is often limited to tertiary centers. In contrast, MRI scanners are widely available, and do not require exposure to radioactive isotopes. Applying network analysis to arterial spin labeling MRI did show some success in identifying PD-related patterns [197, 198], and resting-state functional MRI (rs-fMRI) has shown changes in connectivity in PD patients [199–201]. Principal component analysis has been used to identify a significant PD-related covariance pattern [202] on rs-fMRI, and this has been further refined with independent component analysis [203, 204] to identify an MRI-based PDRP, termed fPDRP [205] (Fig. 36.3). This pattern is characterized by increased activity in the basal ganglia, thalamus, cerebellum/pons, anterior cingulate cortex, and supplementary motor area, with considerable topographic similarity to the PET-derived PDRP. Similar to PDRP, fPDRP expression separates PD patients from healthy controls, its expression correlates with clinical ratings of akinesia-rigidity (but not tremor), and treatment with dopaminergic medication leads to declines in network activity. The same method also identified a cognition-related pattern (fPDCP), which resembles the PET-derived PDCP, with fPDCP expression correlating with

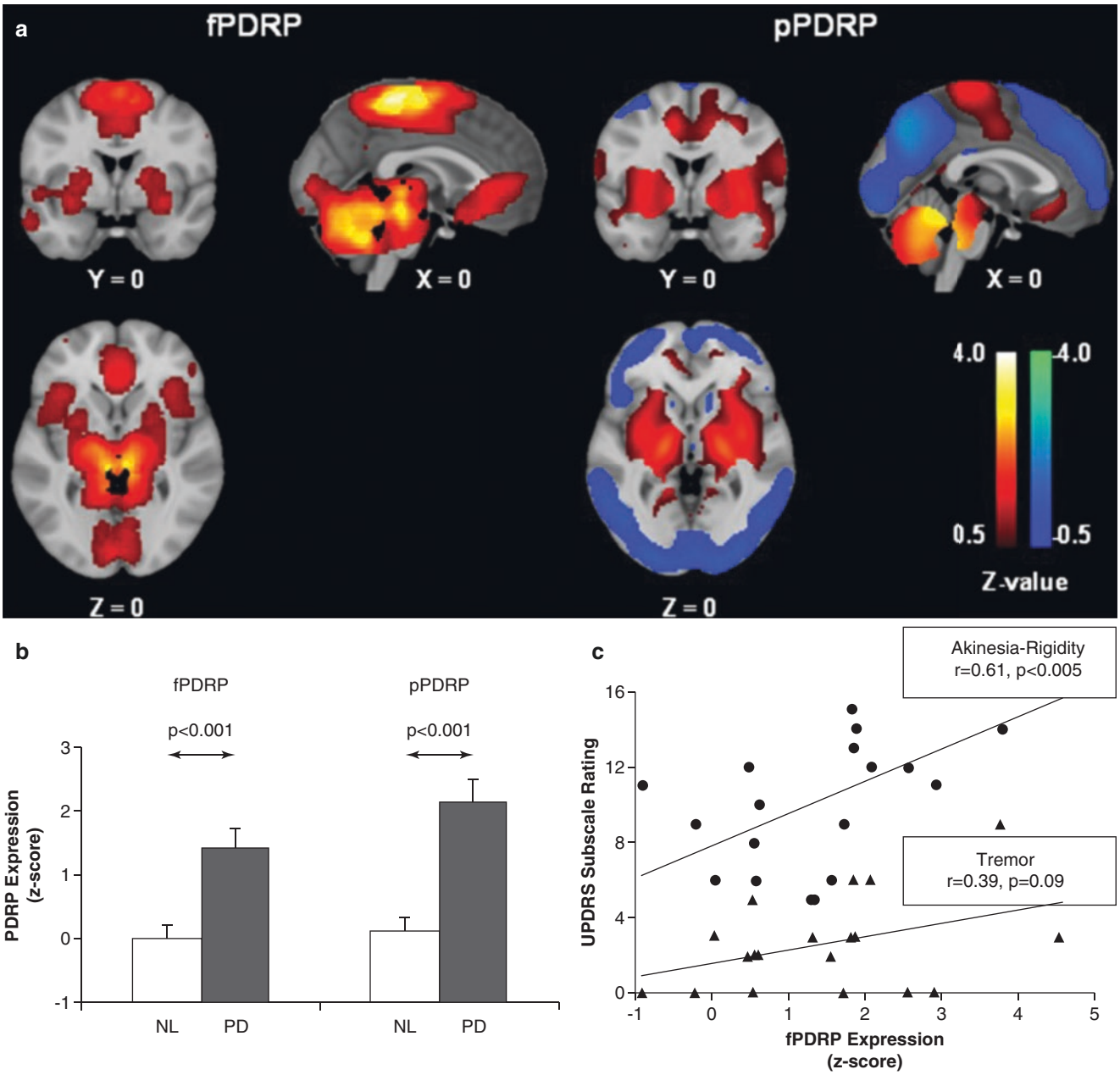

Fig. 36.3 PDRP identified with rs-fMRI. (**a**) PDRP identified in rs-fMRI (fPDRP, left) and PET (pPDRP, right) are shown on the MNI 152 template. fPDRP, derived from 20 normal controls and 20 PD patients, is characterized by increased activity in the basal ganglia, thalamus, cerebellum/pons, anterior cingulate cortex (ACC), and supplementary motor area (SMA). The major network regions that defined the fPDRP corresponded closely to the metabolically active (red areas) regional counterparts of the pPDRP topography. [The color stripes show *Z*-values thresholded at 60.5. Activity increases (fPDRP) or relative metabolic increases (pPDRP) are displayed in red; relative metabolic decreases (pPDRP) are displayed in blue.] (**b**) Expression scores for fPDRP and pPDRP are increased in the PD patients compared to normal controls (NL) ($P < 0.001$; student's *t*-test). [Error bars represent standard errors of the means.] (**c**) fPDRP subject scores correlated with UPDRS ratings for akinesia-rigidity ($r = 0.61$, $P < 0.005$, circles) in the PD subjects scanned at North Shore University Hospital; tremor ratings measured in the same subjects exhibited only a marginal relationship with network expression values ($r = 0.39$, $P = 0.09$, triangles). (Reprinted from Vo et al. [205] with permission from John Wiley and Sons)

verbal learning [205]. Thus, fMRI has the potential to become a noninvasive method for network analysis in PD, though further studies in independent cohorts are needed.

Abnormal Network Architecture of PDRP and PDCP

PDRP does have clinical relevance and reflects underlying pathology, but the biological basis underlying PDRP is not straightforward. For instance, it is not obvious that PDRP represents a distinct brain network of connected areas. This question has been approached using graph theory to analyze functional connections across the brain [122, 206]. Such graph theoretical representation is a topographical schematic based on functional relationships between regions, rather than the functional significance of an area assigned by PDRP. Applying a social network computation to the graphs allows for the delineation of anatomical-functional connections within PDRP and for visualization of enhancing versus competing functional interactions between pairs of nodes [122, 207].

Overall, the PD network exhibits a distinctive core-periphery structure, with a core of dense, mutually facilitating connections between metabolically active nodes in the putamen, globus pallidus, and thalamus, while the periphery contains metabolically less active cortical regions with weaker node-to-node interactions [122]. There is an additional separate module of interconnected, metabolically active nodes involving the cerebellum, pons, frontal cortex, and limbic regions. Organizationally, this PD network is characterized by an exaggeration of the small-world property, i.e., a greater-than-normal number of functional interconnections between nodes within the PDRP space [122]. In general, such small-world properties are thought to achieve efficient information processing at a lower energetic cost [208]. Even in healthy controls, PDRP regions exhibit some degree of this small-world property, reflecting the high information-processing demands on these brain regions. In PD, the increased network small-worldness then is consistent with a maladaptive response to nigrostriatal denervation. Of note, the PD hyperconnectivity is arranged in discrete subnetworks, each of which has been associated with spontaneous oscillatory activity and may mediate distinct clinical features such as bradykinesia-rigidity or tremor [122, 209–211]. These small-world changes were not reversed by clinically effective levodopa treatment, though levodopa does partially normalize the average path length between network nodes to improve information transfer [122].

As in the motor-related networks, graph theory has found increased local connectedness with decreased long-range connections in PD subjects with mild cognitive impairment [212]. These patients showed a marked reduction in the average correlation strength between cortical and subcortical regions compared with healthy controls, demonstrating that even early stages of cognitive decline in PD are associated with disrupted coordination and decreased information-processing efficiency [213].

Differentiating PD from APS

Dopaminergic imaging cannot reliably differentiate between PD and the APS, while in general, metabolic imaging appears superior to dopaminergic imaging in the differentiation of PD and the atypical parkinsonian syndromes [214]. In PD, [^{18}F]-FDG PET imaging reveals hypermetabolism in the basal ganglia, pons, and cerebellum and hypometabolism in the frontal and parietal association areas [125, 126]. In contrast, one of the main findings in APS is hypometabolism in the basal ganglia, coupled with other abnormalities depending on the specific APS [150]. Using voxel-based comparisons between subjects with PD or APS and healthy controls, characteristic patterns for PD and APS can be identified and compared by trained readers prospectively on individual scans [125]. This approach, though, is difficult to scale and does not yield quantifiable measures. Using the SSM/PCA approach (described above for PD), disease-specific metabolic patterns have been identified and validated for the APS [136, 215–217]. The MSA-related pattern (MSARP) is characterized by decreased metabolism in the putamen and cerebellum, while the PSP-related pattern (PSPRP) is characterized by metabolic decreases in the brainstem and medial frontal cortex. The CBD-related patter (CBDRP) exhibits bilateral, asymmetric metabolic reductions involving the frontal and parietal cortex, ipsilateral thalamus, and caudate nucleus.

Such disease-specific covariance networks can easily distinguish between patients and healthy controls, but in order to automatically differentiate among different diseases, multiple patterns need to be utilized [218]. To that end, Tang and colleagues developed a multiple-pattern imaging algorithm that calculates the probability that patients of uncertain clinical diagnosis (at the time of imaging) have PD, MSA, or PSP [219]. Briefly, this algorithm classifies the patient as having PD or APS if certain cutoff criteria for pattern expression is met, followed by second-level analysis to differentiate those subjects with a diagnosis of APS into MSA or PSP. This approach was recently validated in an independent cohort of 129 parkinsonian patients with uncertain diagnosis at the time of imaging [146, 220]. Idiopathic PD subjects were distinguished from APS with 94% specificity and 96% PPV. The algorithm also achieved high accuracy in MSA and PSP. A majority of patients had a disease duration of under 2 years, and diagnostic accuracy was similar in the subjects with shorter symptom duration, underlining the possible utility of this approach even early in the disease course.

Based on a small study, a similar approach can be used to distinguish patients with CBD from those with PSP, though additional steps were required [147, 216]. While PDRP and

MSARP values are elevated predominantly in their respective disease, CBDRP and PSPRP are both abnormally elevated in both CBD and PSP cohorts [147, 216]. So far, CBDRP has not been incorporated into the larger algorithm for PD and APS, and it remains to be seen which (if any) pattern would be elevated in patients with pathologically proven CBD who have different clinical syndromes in life [221–224].

Other automated methods for the differential diagnosis of PD and APS have been reported, such as relevance vector machine analysis [225] and decision trees applied to covariance patterns [226] with some promising results, at least in differentiating PD from APS. Nevertheless, prospective validation studies, preferably comparing these methods in several independent cohorts, are needed before the relative utility of these methods in clinical practice can be judged.

Treatment-Related Network Imaging

PDRP and PDCP expression can decrease with effective PD treatment such as levodopa or DBS though this effect is relatively modest and nonspecific and may be insufficient for clinical trials [149, 163, 164]. Network imaging may prove to be beneficial especially in smaller clinical trials. Accuracy of clinical diagnosis is important for any trial, and clinical trials that use dopaminergic imaging have found that 10–15% of subjects that were clinically categorized as idiopathic PD lack findings of a dopaminergic deficit [55, 77, 227].

Even in a gene therapy trial of advanced PD patients, a significant portion of patients probably did not have PD based on imaging criteria on enrollment [228, 229]. In this phase 2 trial, delivering glutamic acid decarboxylase (*GAD*) into the subthalamic nucleus (STN) of patients with PD had therapeutic effects. Employing OrT/CVA [175], it was found that those who received AAV2-*GAD* gene therapy developed a unique treatment-dependent polysynaptic brain circuit, termed the *GAD*-related pattern (GADRP), which reflected the formation of new polysynaptic functional pathways linking the STN to motor cortical regions [230].

Lastly, placebo effects can be a particularly prominent confounder in PD trials, with 16% of PD subjects randomized to placebo demonstrating >50% improvement in motor ratings in a review of placebo-controlled PD trials [231]. In the same gene therapy trial, Ko and colleagues were able to identify and validate a specific metabolic brain network associated with the placebo response in PD. This sham surgery-related pattern primarily involved anatomical-functional pathways linking the posterior cerebellar vermis to the limbic cortex via the ventral anterior thalamus, amygdala, and caudate nucleus [165]. Baseline network expression, which was measured prior to randomization, correlated with the motor response that was subsequently observed under blinded trial conditions in the sham group. These network changes did not appear following the experimental subthalamic nucleus AAV2-*GAD* gene therapy, and they were reversed by unblinding. Future studies will be needed to determine if this sham surgery-related pattern is universal to PD or unique to this trial.

Another group using fMRI also showed that the placebo response in PD involves a complex network of regions beyond the striatum [232]. In this study an expensive placebo produced a stronger response than a cheap placebo, deactivating the left putamen, sensorimotor cortices, and premotor cortex, whereas the cheaper placebo activated the bilateral anterior and posterior cingulate cortices, left lateral sensorimotor cortex, and right parietal cortex, among other regions.

Other Functional Imaging

Serotonergic Imaging

Functional imaging studies have used radioligands such as [^{11}C](+)McN5652 and [^{11}C]-3-amino-4-(2-dimethylaminomethylphenylthio)-benzonitrile ([^{11}C]-DASB) to assess the function of the serotonin transporter (SERT) in the brain of patients with PD [233–235]. An early study found decreased [^{11}C](+)McN5652 binding in the putamen and caudate nucleus of PD patients bilaterally, which correlated with disease severity as assessed by the Hoehn-Yahr Scale (HYS) [234]. [^{11}C]-DASB PET studies have repeatedly demonstrated widespread, symmetric reductions in SERT uptake in the forebrain, striatum, and brainstem, with relative sparing of the caudal brainstem raphe nuclei in early PD [233, 235, 236]. Specifically, regional analysis of [^{11}C]-DASB uptake indicated decreased SERT binding in the caudate nucleus, thalamus, hypothalamus, and anterior cingulate in early disease; additional reductions in the putamen, insular cortex, posterior cingulate, and prefrontal cortex in established cases; and further reduced values in the ventral striatum, raphe nuclei, and amygdala in advanced disease. Decreased [^{11}C]-DASB binding did not correlate to UPDRS scores, Hoehn and Yahr staging, disease duration, or level of exposure to dopaminergic therapy, indicating that involvement of the serotonergic system is most reflected in non-motor PD symptoms [233, 235].

Indeed, relatively higher [^{11}C]-DASB binding in the raphe and limbic structures (reflecting lower extracellular serotonin levels) has been found to correlate with depressive symptoms in PD [237]. Similarly, apathetic parkinsonian patients display greater serotonergic alteration in the ventral striatum, dorsal and subgenual parts of the anterior cingulate, as well as the right caudate nucleus and right orbitofrontal cortex, compared to non-apathetic PD patients [238]. The severity of apathy was mainly related to specific serotonergic lesions within the right anterior caudate nucleus and orbitofrontal cortex, while the degree of both depression and anxi-

ety was primarily linked to serotonergic disruption within the bilateral subgenual and/or right dorsal anterior cingulate cortex. In this study, dopaminergic degeneration did not correlate with apathy, anxiety, or depression [238]. Another study found PD patients with sleep dysfunction to have lower [^{11}C]-DASB binding in the caudate, putamen, ventral striatum, thalamus, hypothalamus, and raphe nuclei, compared to PD without sleep dysfunction [239].

Serotonin may, nevertheless, be involved in some motor symptoms. A [^{11}C]-WAY-100635 PET study assessed binding to serotonergic 5-HT(1A) receptors in PD patients demonstrated significant reductions in midbrain raphe 5-HT(1A) uptake compared to controls, and in these patients, the level of midbrain [^{11}C]-WAY-100635 binding correlated with UPDRS composite tremor scores, but not rigidity or bradykinesia [240]. Likewise, studies using [^{11}C]-DASB and [^{11}C]-raclopride found that striatal serotonergic terminals may contribute to the development of levodopa-induced dyskinesias via aberrant levodopa processing [241–243].

[^{123}I]-FP-CIT, which is used for imaging of the dopamine transporter system, also exhibits binding to the SERT system (with a DaT/SERT selectivity of 2.8 [244, 245]) and may be useful to detect differences in predominantly serotonergic brain regions between PD and DLB, although this has not been studied prospectively [246, 247].

Using a different SERT radiotracer and PET imaging, [^{11}C]-MADAM, Fazio and colleagues did not find statistically significant regional differences between early PD patients and healthy controls, though there was a trend towards reduced SERT availability in the caudate, putamen, and pallidus, with no difference in the raphe nuclei [248]. This did not change on a 2-year follow-up, but using network analysis, they found a progressive disconnection of the raphe nuclei and cortical and subcortical regions, suggesting that the serotonergic system may play a role in network dysregulation.

Microglial Activation

Neuroinflammation associated with increased microglial activation is present in PD and the various APS [249–252], suggesting that activated microglia may play a role in the pathogenesis of these disorders. [^{11}C](R)-PK11195 is a specific ligand for the mitochondrial translocator protein18 kDa (TSPO, previously also known as the peripheral benzodiazepine binding site, PBBS) which is highly expressed in activated microglial cells [253]. Though specific for TSPO, [^{11}C]-(R)-PK11195 exhibits a low signal-to-noise ratio. To overcome this, several TSPO radioligands with improved signal have recently been described, including [^{11}C]-PBR28, [^{11}C]-DPA713, [^{18}F]-FEPPA, and [^{11}C]-DAA1106 [254, 255].

In a 6-hydroxydopamine (6-OHDA)-induced PD rat model, increased [^{11}C](R)-PK11195 binding is seen in the substantia nigra and striatum, indicating marked microglial activation in these areas, which was further confirmed by postmortem immunohistochemical evidence of regional neuroinflammation [256]. Using a second generation TSPO radioligand, [^{11}C]-PBR28, Real and colleagues found increased tracer uptake in the striatum 10 days after 6-OHDA injection. This increase, however, reversed by 30 days, suggesting that the microglial activation is an acute process accompanying nigral neurodegeneration [257].

In advanced PD, widespread microglial activation has been documented involving the meso-basal ganglia, thalamocortical loop, and extrastriatal regions, indicating that neuroinflammation persists as the disease progresses [258–260]. TSPO binding levels, however, are not correlated with clinical severity of striatal FDOPA uptake and remain stable over time. This contrasts with early drug-naive PD, where the level of [^{11}C](R)-PK11195 uptake in the midbrain contralateral to the clinically affected side correlated with the severity of motor symptoms and inversely with DaT binding ([^{11}C]-CFT uptake) in the striatum [259]. In PD patients with and without dementia, [^{11}C]-(R)-PK11195 binding correlated with lower cognitive scores and cortical hypometabolism [261, 262].

Since neuroinflammation and accompanying microglial activation may contribute to the early neurodegenerative process in PD; theoretically, early treatment with anti-inflammatory or neuroprotective drugs might be beneficial [263]. This hypothesis was explored in a small pilot study of [^{11}C](R)-PK11195 PET imaging in five PD patients treated with celecoxib [264]. This did not result in significant post-treatment changes in the putamen and midbrain binding in this small sample, suggesting that the neuroinflammation in PD is not easily altered by conventional anti-inflammatory therapy.

However, it must be noted that at least one study with [^{11}C]-PBR28 in 16 PD patients could not demonstrate increased TSPO binding or any relationship between TSPO binding and DAT binding [254]. Studies with both [^{11}C]-PBR28 and [^{18}F]-FEPPA suggest that TSPO polymorphisms strongly influence ligand binding, which ultimately may limit the utility of these tracers as biomarkers in parkinsonian disorders [265–268].

Conclusion

In this chapter, we have briefly reviewed recent advances in MRI, SPECT, and PET imaging in Parkinson's disease. Dopaminergic imaging correlates with the underlying pathology of PD and may be helpful in imaging preclinical PD; however, there is overlap in dopaminergic dysfunction between PD and other degenerative parkinsonism. Using metabolic imaging and network approaches has led to insight

into the more widespread dysfunction in PD, and some of the biological underpinnings related to that dysfunction. Moreover, metabolic imaging has been proven to aid in the differential diagnosis of PD and APS, even early in the disease course. Metabolic imaging has been incorporated into at least one clinical trial, aiding with accurate diagnosis at enrollment and shedding light on the response to treatment and placebo. MR imaging, in particular fMRI, may be able to replace the more invasive nuclear medicine imaging techniques, but further prospective studies are needed.

References

1. Lees AJ, Hardy J, Revesz T. Parkinson's disease. Lancet. 2009;373(9680):2055–66.
2. Poewe W, et al. Parkinson disease. Nat Rev Dis Primers. 2017;3:17013.
3. Twelves D, Perkins KS, Counsell C. Systematic review of incidence studies of Parkinson's disease. Mov Disord. 2003;18(1):19–31.
4. Van Den Eeden SK, et al. Incidence of Parkinson's disease: variation by age, gender, and race/ethnicity. Am J Epidemiol. 2003;157(11):1015–22.
5. Kusumi M, et al. Epidemiology of Parkinson's disease in Yonago City, Japan: comparison with a study carried out 12 years ago. Neuroepidemiology. 1996;15(4):201–7.
6. Aharon-Peretz J, Rosenbaum H, Gershoni-Baruch R. Mutations in the glucocerebrosidase gene and Parkinson's disease in Ashkenazi Jews. N Engl J Med. 2004;351(19):1972–7.
7. Ozelius LJ, et al. LRRK2 G2019S as a cause of Parkinson's disease in Ashkenazi Jews. N Engl J Med. 2006;354(4):424–5.
8. Yahalom G, et al. Carriers of both GBA and LRRK2 mutations, compared to carriers of either, in Parkinson's disease: risk estimates and genotype-phenotype correlations. Parkinsonism Relat Disord. 2019;62:179–84.
9. Braak H, Del Tredici K. Neuroanatomy and pathology of sporadic Parkinson's disease. Adv Anat Embryol Cell Biol. 2009;201:1–119.
10. Halliday GM, McCann H. The progression of pathology in Parkinson's disease. Ann N Y Acad Sci. 2010;1184:188–95.
11. Dickson DW, et al. Neuropathological assessment of Parkinson's disease: refining the diagnostic criteria. Lancet Neurol. 2009;8(12):1150–7.
12. Hughes A, et al. The accuracy of diagnosis of Parkinsonian syndromes in a specialist movement disorder service. Brain. 2002;125(Pt 4):861–70.
13. Postuma RB, et al. MDS clinical diagnostic criteria for Parkinson's disease. Mov Disord. 2015;30(12):1591–601.
14. Berg D, et al. MDS research criteria for prodromal Parkinson's disease. Mov Disord. 2015;30(12):1600–11.
15. Fahn S, et al. Levodopa and the progression of Parkinson's disease. N Engl J Med. 2004;351(24):2498–508.
16. Rizzo G, et al. Accuracy of clinical diagnosis of Parkinson disease: a systematic review and meta-analysis. Neurology. 2016;86(6):566–76.
17. Mahlknecht P, et al. Significance of MRI in diagnosis and differential diagnosis of Parkinson's disease. Neurodegener Dis. 2010;7(5):300–18.
18. Seppi K, Schocke M. An update on conventional and advanced magnetic resonance imaging techniques in the differential diagnosis of neurodegenerative Parkinsonism. Curr Opin Neurol. 2005;18(4):370–5.
19. Vizcarra JA, et al. Vascular Parkinsonism: deconstructing a syndrome. Mov Disord. 2015;30(7):886–94.
20. Blazejewska AI, et al. Visualization of nigrosome 1 and its loss in PD: pathoanatomical correlation and in vivo 7 T MRI. Neurology. 2013;81(6):534–40.
21. Schwarz ST, et al. The 'swallow tail' appearance of the healthy nigrosome - a new accurate test of Parkinson's disease: a case-control and retrospective cross-sectional MRI study at 3T. PLoS One. 2014;9(4):e93814.
22. Kim JM, et al. Loss of substantia nigra hyperintensity on 7 Tesla MRI of Parkinson's disease, multiple system atrophy, and progressive supranuclear palsy. Parkinsonism Relat Disord. 2016;26:47–54.
23. Mahlknecht P, et al. Meta-analysis of dorsolateral nigral hyperintensity on magnetic resonance imaging as a marker for Parkinson's disease. Mov Disord. 2017;32(4):619–23.
24. Sung YH, et al. Drug-induced Parkinsonism versus idiopathic Parkinson disease: utility of Nigrosome 1 with 3-T imaging. Radiology. 2016;279(3):849–58.
25. Rizzo G, et al. Loss of swallow tail sign on susceptibility-weighted imaging in dementia with Lewy bodies. J Alzheimers Dis. 2019;67(1):61–5.
26. Bae YJ, et al. Loss of nigral hyperintensity on 3 tesla MRI of Parkinsonism: comparison with (123) I-FP-CIT SPECT. Mov Disord. 2016;31(5):684–92.
27. Vaillancourt DE, et al. High-resolution diffusion tensor imaging in the substantia nigra of de novo Parkinson disease. Neurology. 2009;72(16):1378–84.
28. Feng JY, et al. The putaminal abnormalities on 3.0T magnetic resonance imaging: can they separate parkinsonism-predominant multiple system atrophy from Parkinson's disease? Acta Radiol. 2015;56(3):322–8.
29. Pradhan S, Tandon R. Relevance of non-specific MRI features in multiple system atrophy. Clin Neurol Neurosurg. 2017;159:29–33.
30. Mueller C, et al. The diagnostic accuracy of the hummingbird and morning glory sign in patients with neurodegenerative parkinsonism. Parkinsonism Relat Disord. 2018;54:90–4.
31. Eraslan C, et al. MRI evaluation of progressive supranuclear palsy: differentiation from Parkinson's disease and multiple system atrophy. Neurol Res. 2019;41(2):110–7.
32. Portet M, Filyridou M, Howlett DC. Hot cross bun sign. J Neurol. 2019;266(10):2573–4.
33. Way C, Pettersson D, Hiller A. The 'Hot cross Bun' sign is not always multiple system atrophy: etiologies of 11 cases. J Mov Disord. 2019;12(1):27–30.
34. Izawa MO, et al. Combination of transcranial sonography, olfactory testing, and MIBG myocardial scintigraphy as a diagnostic indicator for Parkinson's disease. Eur J Neurol. 2012;19(3):411–6.
35. Walter U, et al. Transcranial brain sonography findings in discriminating between parkinsonism and idiopathic Parkinson disease. Arch Neurol. 2007;64(11):1635–40.
36. Berg D, Godau J, Walter U. Transcranial sonography in movement disorders. Lancet Neurol. 2008;7(11):1044–55.
37. Gaenslen A, et al. The specificity and sensitivity of transcranial ultrasound in the differential diagnosis of Parkinson's disease: a prospective blinded study. Lancet Neurol. 2008;7(5):417–24.
38. Li DH, et al. Diagnostic accuracy of transcranial sonography of the substantia Nigra in Parkinson's disease: a systematic review and meta-analysis. Sci Rep. 2016;6:20863.
39. Zhou HY, et al. Substantia nigra echogenicity associated with clinical subtypes of Parkinson's disease. J Parkinsons Dis. 2018;8(2):333–40.
40. Tao A, et al. Accuracy of transcranial sonography of the substantia Nigra for detection of Parkinson's disease: a systematic review and Meta-analysis. Ultrasound Med Biol. 2019;45(3):628–41.

41. Stern MB. Transcranial ultrasound in Parkinson's disease. Lancet Neurol. 2008;7(5):376–8.
42. Walter U. Transcranial brain sonography findings in Parkinson's disease: implications for pathogenesis, early diagnosis and therapy. Expert Rev Neurother. 2009;9(6):835–46.
43. Zhou HY, et al. The role of substantia nigra sonography in the differentiation of Parkinson's disease and multiple system atrophy. Transl Neurodegener. 2018;7:15.
44. Busse K, et al. Value of combined midbrain sonography, olfactory and motor function assessment in the differential diagnosis of early Parkinson's disease. J Neurol Neurosurg Psychiatry. 2012;83(4):441–7.
45. Berg D, et al. Enlarged hyperechogenic substantia nigra as a risk marker for Parkinson's disease. Mov Disord. 2013;28(2):216–9.
46. Mahlknecht P, et al. Midbrain hyperechogenicity, hyposmia, mild Parkinsonian signs and risk for incident Parkinson's disease over 10 years: a prospective population-based study. Parkinsonism Relat Disord. 2020;70:51–4.
47. Dhawan V, Eidelberg D. PET imaging in Parkinson's disease and other neurodegenerative disorders. In: Gilman S, editor. Neurobiology of disease. San Diego: Academic Press; 2007. p. 821–8.
48. Calabria FF, et al. Current status and future challenges of brain imaging with (18)F-DOPA PET for movement disorders. Hell J Nucl Med. 2016;19(1):33–41.
49. Lee CS, et al. In vivo positron emission tomographic evidence for compensatory changes in presynaptic dopaminergic nerve terminals in Parkinson's disease. Ann Neurol. 2000;47(4):493–503.
50. Bruck A, et al. A follow-up study on 6-[18F]fluoro-L-dopa uptake in early Parkinson's disease shows nonlinear progression in the putamen. Mov Disord. 2009;24(7):1009–15.
51. Sossi V, et al. Increase in dopamine turnover occurs early in Parkinson's disease: evidence from a new modeling approach to PET 18 F-fluorodopa data. J Cereb Blood Flow Metab. 2002;22(2):232–9.
52. Sossi V, et al. Changes of dopamine turnover in the progression of Parkinson's disease as measured by positron emission tomography: their relation to disease-compensatory mechanisms. J Cereb Blood Flow Metab. 2004;24(8):869–76.
53. Nandhagopal R, McKeown MJ, Stoessl AJ. Functional imaging in Parkinson disease. Neurology. 2008;70(16 Pt 2):1478–88.
54. de la Fuente-Fernandez R, et al. Visualizing vesicular dopamine dynamics in Parkinson's disease. Synapse. 2009;63(8):713–6.
55. Marek KI, Seibyl J, Parkinson Study Group. β-CIT scans without evidence of dopaminergic deficit (SWEDD) in the ELLDOPA-CIT and CALM-CIT study: long-term imaging assessment. Neurology. 2003;60(Suppl. 1):A293.
56. Booij J, et al. [123I]FP-CIT SPECT shows a pronounced decline of striatal dopamine transporter labelling in early and advanced Parkinson's disease. J Neurol Neurosurg Psychiatry. 1997;62(2):133–40.
57. Rinne JO, et al. PET examination of the monoamine transporter with [11C]beta-CIT and [11C]beta-CFT in early Parkinson's disease. Synapse. 1995;21(2):97–103.
58. Guttman M, et al. [11C]RTI-32 PET studies of the dopamine transporter in early dopa-naive Parkinson's disease: implications for the symptomatic threshold. Neurology. 1997;48(6):1578–83.
59. Frost JJ, et al. Positron emission tomographic imaging of the dopamine transporter with 11C-WIN 35,428 reveals marked declines in mild Parkinson's disease. Ann Neurol. 1993;34(3):423–31.
60. Ribeiro MJ, et al. A multitracer dopaminergic PET study of young-onset Parkinsonian patients with and without parkin gene mutations. J Nucl Med. 2009;50(8):1244–50.
61. Leenders KL, et al. The nigrostriatal dopaminergic system assessed in vivo by positron emission tomography in healthy volunteer subjects and patients with Parkinson's disease. Arch Neurol. 1990;47(12):1290–8.
62. Kagi G, Bhatia KP, Tolosa E. The role of DAT-SPECT in movement disorders. J Neurol Neurosurg Psychiatry. 2010;81(1):5–12.
63. Bajaj N, Hauser RA, Grachev ID. Clinical utility of dopamine transporter single photon emission CT (DaT-SPECT) with (123I) ioflupane in diagnosis of Parkinsonian syndromes. J Neurol Neurosurg Psychiatry. 2013;84(11):1288–95.
64. Thobois S, et al. What a neurologist should know about PET and SPECT functional imaging for Parkinsonism: a practical perspective. Parkinsonism Relat Disord. 2019;59:93–100.
65. Koeppe RA, et al. 11C-DTBZ and 18F-FDG PET measures in differentiating dementias. J Nucl Med. 2005;46(6):936–44.
66. Jin S, et al. Differential diagnosis of Parkinsonism using dual-phase F-18 FP-CIT PET imaging. Nucl Med Mol Imaging. 2013;47(1):44–51.
67. Jin S, et al. Additional value of early-phase 18F-FP-CIT PET image for differential diagnosis of atypical Parkinsonism. Clin Nucl Med. 2017;42(2):e80–7.
68. Broussolle E, et al. The relation of putamen and caudate nucleus 18F-Dopa uptake to motor and cognitive performances in Parkinson's disease. J Neurol Sci. 1999;166(2):141–51.
69. Vingerhoets FJ, et al. Which clinical sign of Parkinson's disease best reflects the nigrostriatal lesion? Ann Neurol. 1997;41(1):58–64.
70. Nurmi E, et al. Rate of progression in Parkinson's disease: a 6-[18F] fluoro-L-dopa PET study. Mov Disord. 2001;16(4):608–15.
71. Tang CC, et al. Abnormalities in metabolic network activity precede the onset of motor symptoms in Parkinson's disease. J Neurosci. 2010;30(3):1049–56.
72. Nurmi E, et al. Progression in Parkinson's disease: a positron emission tomography study with a dopamine transporter ligand [18F]CFT. Ann Neurol. 2000;47(6):804–8.
73. Asenbaum S, et al. Imaging of dopamine transporters with iodine-123-beta-CIT and SPECT in Parkinson's disease. J Nucl Med. 1997;38(1):1–6.
74. Marek KL, et al. [123I] beta-CIT/SPECT imaging demonstrates bilateral loss of dopamine transporters in hemi-Parkinson's disease. Neurology. 1996;46(1):231–7.
75. Baucknehtt M, et al. Presynaptic dopaminergic neuroimaging in REM sleep behavior disorder: a systematic review and meta-analysis. Sleep Med Rev. 2018;41:266–74.
76. Marek K, et al. [123I]beta-CIT SPECT imaging assessment of the rate of Parkinson's disease progression. Neurology. 2001;57(11):2089–94.
77. Whone AL, et al. Slower progression of Parkinson's disease with ropinirole versus levodopa: the REAL-PET study. Ann Neurol. 2003;54(1):93–101.
78. Hauser RA, et al. Long-term evaluation of bilateral fetal nigral transplantation in Parkinson disease. Arch Neurol. 1999;56(2):179–87.
79. Piccini P, et al. Dopamine release from nigral transplants visualized in vivo in a Parkinson's patient. Nat Neurosci. 1999;2(12):1137–40.
80. Freed CR, et al. Transplantation of embryonic dopamine neurons for severe Parkinson's disease. N Engl J Med. 2001;344(10):710–9.
81. Piccini P, et al. Factors affecting the clinical outcome after neural transplantation in Parkinson's disease. Brain. 2005;128(Pt 12):2977–86.
82. Olanow CW, et al. A double-blind controlled trial of bilateral fetal nigral transplantation in Parkinson's disease. Ann Neurol. 2003;54(3):403–14.
83. Parkinson Study Group. Dopamine transporter brain imaging to assess the effects of pramipexole vs levodopa on Parkinson disease progression. JAMA. 2002;287(13):1653–61.

84. Marshall VL, et al. Two-year follow-up in 150 consecutive cases with normal dopamine transporter imaging. Nucl Med Commun. 2006;27(12):933–7.
85. Marek K, et al. Longitudinal follow-up of SWEDD subjects in the PRECEPT study. Neurology. 2014;82(20):1791–7.
86. Eckert T, et al. Regional metabolic changes in Parkinsonian patients with normal dopaminergic imaging. Mov Disord. 2007;22(2):167–73.
87. Jennings DL, et al. (123I) beta-CIT and single-photon emission computed tomographic imaging vs clinical evaluation in Parkinsonian syndrome: unmasking an early diagnosis. Arch Neurol. 2004;61(8):1224–9.
88. Benamer HT, et al. Prospective study of presynaptic dopaminergic imaging in patients with mild parkinsonism and tremor disorders: part 1. Baseline and 3-month observations. Mov Disord. 2003;18(9):977–84.
89. Rinne JO, et al. PET demonstrates different behaviour of striatal dopamine D-1 and D-2 receptors in early Parkinson's disease. J Neurosci Res. 1990;27(4):494–9.
90. Cropley VL, et al. Pre- and post-synaptic dopamine imaging and its relation with frontostriatal cognitive function in Parkinson disease: PET studies with [11C]NNC 112 and [18F] FDOPA. Psychiatry Res. 2008;163(2):171–82.
91. Pirker W, et al. Iodine-123-epidepride-SPECT: studies in Parkinson's disease, multiple system atrophy and Huntington's disease. J Nucl Med. 1997;38(11):1711–7.
92. Verstappen CC, et al. Diagnostic value of asymmetric striatal D2 receptor upregulation in Parkinson's disease: an [123I]IBZM and [123I]FP-CIT SPECT study. Eur J Nucl Med Mol Imaging. 2007;34(4):502–7.
93. Rinne JO, et al. Increased density of dopamine D2 receptors in the putamen, but not in the caudate nucleus in early Parkinson's disease: a PET study with [11C]raclopride. J Neurol Sci. 1995;132(2):156–61.
94. Kaasinen V, et al. Upregulation of putaminal dopamine D2 receptors in early Parkinson's disease: a comparative PET study with [11C] raclopride and [11C]N-methylspiperone. J Nucl Med. 2000;41(1):65–70.
95. Antonini A, et al. Long-term changes of striatal dopamine D2 receptors in patients with Parkinson's disease: a study with positron emission tomography and [11C]raclopride. Mov Disord. 1997;12(1):33–8.
96. Thobois S, et al. Role of dopaminergic treatment in dopamine receptor down-regulation in advanced Parkinson disease: a positron emission tomographic study. Arch Neurol. 2004;61(11):1705–9.
97. Cardenas L, et al. Oral D-amphetamine causes prolonged displacement of [11C]raclopride as measured by PET. Synapse. 2004;51(1):27–31.
98. Innis RB, et al. Amphetamine-stimulated dopamine release competes in vivo for [123I]IBZM binding to the D2 receptor in nonhuman primates. Synapse. 1992;10(3):177–84.
99. de la Fuente-Fernandez R, et al. Expectation and dopamine release: mechanism of the placebo effect in Parkinson's disease. Science. 2001;293(5532):1164–6.
100. Piccini P, Pavese N, Brooks DJ. Endogenous dopamine release after pharmacological challenges in Parkinson's disease. Ann Neurol. 2003;53(5):647–53.
101. Niccolini F, Su P, Politis M. Dopamine receptor mapping with PET imaging in Parkinson's disease. J Neurol. 2014;261(12):2251–63.
102. Strafella AP, et al. Corticostriatal functional interactions in Parkinson's disease: a rTMS/[11C]raclopride PET study. Eur J Neurosci. 2005;22(11):2946–52.
103. Pavese N, et al. Clinical correlates of levodopa-induced dopamine release in Parkinson disease: a PET study. Neurology. 2006;67(9):1612–7.
104. de La Fuente-Fernandez R, et al. Apomorphine-induced changes in synaptic dopamine levels: positron emission tomography evidence for presynaptic inhibition. J Cereb Blood Flow Metab. 2001;21(10):1151–9.
105. de la Fuente-Fernandez R, et al. Biochemical variations in the synaptic level of dopamine precede motor fluctuations in Parkinson's disease: PET evidence of increased dopamine turnover. Ann Neurol. 2001;49(3):298–303.
106. de la Fuente-Fernandez R, et al. Levodopa-induced changes in synaptic dopamine levels increase with progression of Parkinson's disease: implications for dyskinesias. Brain. 2004;127(Pt 12):2747–54.
107. Jourdain VA, et al. Levodopa-induced changes in neurovascular reactivity in Parkinson's disease. Mov Disord. 2015;30(Suppl 1):S11.
108. Jourdain VA, et al. Increased putamen hypercapnic vasoreactivity in levodopa-induced dyskinesia. JCI Insight. 2017;2(20):96411.
109. Lerner RP, et al. Levodopa-induced abnormal involuntary movements correlate with altered permeability of the blood-brain-barrier in the basal ganglia. Sci Rep. 2017;7(1):16005.
110. Evans AH, et al. Compulsive drug use linked to sensitized ventral striatal dopamine transmission. Ann Neurol. 2006;59(5):852–8.
111. Steeves TD, et al. Increased striatal dopamine release in Parkinsonian patients with pathological gambling: a [11C] raclopride PET study. Brain. 2009;132(Pt 5):1376–85.
112. O'Sullivan SS, et al. Cue-induced striatal dopamine release in Parkinson's disease-associated impulsive-compulsive behaviours. Brain. 2011;134(Pt 4):969–78.
113. Leenders KL. Significance of non-presynaptic SPECT tracer methods in Parkinson's disease. Mov Disord. 2003;18(Suppl 7):S39–42.
114. Kim YJ, et al. Combination of dopamine transporter and D2 receptor SPECT in the diagnostic evaluation of PD, MSA, and PSP. Mov Disord. 2002;17(2):303–12.
115. Knudsen GM, et al. Imaging of dopamine transporters and D2 receptors in patients with Parkinson's disease and multiple system atrophy. Eur J Nucl Med Mol Imaging. 2004;31(12):1631–8.
116. Klaffke S, et al. Dopamine transporters, D2 receptors, and glucose metabolism in corticobasal degeneration. Mov Disord. 2006;21(10):1724–7.
117. Plotkin M, et al. Combined 123I-FP-CIT and 123I-IBZM SPECT for the diagnosis of parkinsonian syndromes: study on 72 patients. J Neural Transm (Vienna). 2005;112(5):677–92.
118. Vlaar AM, et al. Diagnostic value of 123I-ioflupane and 123I-iodobenzamide SPECT scans in 248 patients with parkinsonian syndromes. Eur Neurol. 2008;59(5):258–66.
119. Sudmeyer M, et al. Diagnostic accuracy of combined FP-CIT, IBZM, and MIBG scintigraphy in the differential diagnosis of degenerative parkinsonism: a multidimensional statistical approach. J Nucl Med. 2011;52(5):733–40.
120. Eidelberg D. Metabolic brain networks in neurodegenerative disorders: a functional imaging approach. Trends Neurosci. 2009;32(10):548–57.
121. Caminiti SP, et al. Metabolic connectomics targeting brain pathology in dementia with Lewy bodies. J Cereb Blood Flow Metab. 2017;37(4):1311–25.
122. Ko JH, Spetsieris PG, Eidelberg D. Network structure and function in Parkinson's disease. Cereb Cortex. 2018;28(12):4121–35.
123. Sala A, et al. Altered brain metabolic connectivity at multiscale level in early Parkinson's disease. Sci Rep. 2017;7(1):4256.
124. Spetsieris PG, et al. Metabolic resting-state brain networks in health and disease. Proc Natl Acad Sci U S A. 2015;112(8):2563–8.
125. Eckert T, et al. FDG PET in the differential diagnosis of Parkinsonian disorders. NeuroImage. 2005;26(3):912–21.

126. Booij J, Teune LK, Verberne HJ. The role of molecular imaging in the differential diagnosis of Parkinsonism. Q J Nucl Med Mol Imaging. 2012;56(1):17–26.
127. Woo CW, et al. Building better biomarkers: brain models in translational neuroimaging. Nat Neurosci. 2017;20(3):365–77.
128. Gordon E, Rohrer JD, Fox NC. Advances in neuroimaging in frontotemporal dementia. J Neurochem. 2016;138(Suppl 1):193–210.
129. Nicastro N, et al. Classification of degenerative Parkinsonism subtypes by support-vector-machine analysis and striatal (123)I-FP-CIT indices. J Neurol. 2019;266(7):1771–81.
130. Niethammer M, Eidelberg D. Metabolic brain networks in translational neurology: concepts and applications. Ann Neurol. 2012;72(5):635–47.
131. Pievani M, et al. Brain connectivity in neurodegenerative diseases--from phenotype to proteinopathy. Nat Rev Neurol. 2014;10(11):620–33.
132. Surmeier DJ, Obeso JA, Halliday GM. Selective neuronal vulnerability in Parkinson disease. Nat Rev Neurosci. 2017;18(2):101–13.
133. Tang CC, et al. Metabolic network as a progression biomarker of premanifest huntington's disease. J Clin Invest. 2013;123(9):4076–88.
134. Titov D, et al. Metabolic connectivity for differential diagnosis of dementing disorders. J Cereb Blood Flow Metab. 2017;37(1):252–62.
135. Eckert T, Edwards C. The application of network mapping in differential diagnosis of Parkinsonian disorders. Clin Neurosci Res. 2007;6:359–66.
136. Eckert T, et al. Abnormal metabolic networks in atypical Parkinsonism. Mov Disord. 2008;23(5):727–33.
137. Feigin A, et al. Thalamic metabolism and symptom onset in preclinical Huntington's disease. Brain. 2007;130(Pt 11):2858–67.
138. Huang C, et al. Metabolic brain networks associated with cognitive function in Parkinson's disease. NeuroImage. 2007;34(2):714–23.
139. Habeck C, et al. Multivariate and univariate neuroimaging biomarkers of Alzheimer's disease. NeuroImage. 2008;40(4):1503–15.
140. Habeck C, Stern Y, Alzheimer's Disease Neuroimaging Initiative. Multivariate data analysis for neuroimaging data: overview and application to Alzheimer's disease. Cell Biochem Biophys. 2010;58(2):53–67.
141. Spetsieris PG, Eidelberg D. Scaled subprofile modeling of resting state imaging data in Parkinson's disease: methodological issues. NeuroImage. 2011;54(4):2899–914.
142. Eckert T, Tang C, Eidelberg D. Assessment of the progression of Parkinson's disease: a metabolic network approach. Lancet Neurol. 2007;6(10):926–32.
143. Teune LK, et al. Validation of Parkinsonian disease-related metabolic brain patterns. Mov Disord. 2013;28(4):547–51.
144. Wu P, et al. Metabolic brain network in the Chinese patients with Parkinson's disease based on 18F-FDG PET imaging. Parkinsonism Relat Disord. 2013;19(6):622–7.
145. Holtbernd F, et al. Dopaminergic correlates of metabolic network activity in Parkinson's disease. Hum Brain Mapp. 2015;36(9):3575–85.
146. Tripathi M, et al. Automated differential diagnosis of early Parkinsonism using metabolic brain networks: a validation study. J Nucl Med. 2016;57(1):60–6.
147. Ko JH, Lee CS, Eidelberg D. Metabolic network expression in Parkinsonism: clinical and dopaminergic correlations. J Cereb Blood Flow Metab. 2017;37(2):683–93.
148. Tomse P, et al. Abnormal metabolic brain network associated with Parkinson's disease: replication on a new European sample. Neuroradiology. 2017;59(5):507–15.
149. Asanuma K, et al. Network modulation in the treatment of Parkinson's disease. Brain. 2006;129(Pt 10):2667–78.
150. Schindlbeck KA, Eidelberg D. Network imaging biomarkers: insights and clinical applications in Parkinson's disease. Lancet Neurol. 2018;17(7):629–40.
151. Schindlbeck KA, et al. Metabolic network abnormalities in drug-naive Parkinson's disease. Mov Disord. 2020;35(4):587–94.
152. Ma Y, et al. Abnormal metabolic network activity in Parkinson's disease: test-retest reproducibility. J Cereb Blood Flow Metab. 2007;27(3):597–605.
153. Hirano S, et al. Dissociation of metabolic and neurovascular responses to levodopa in the treatment of Parkinson's disease. J Neurosci. 2008;28(16):4201–9.
154. Ma Y, Eidelberg D. Functional imaging of cerebral blood flow and glucose metabolism in Parkinson's disease and Huntington's disease. Mol Imaging Biol. 2007;9(4):223–33.
155. Eckert T, et al. Quantification of Parkinson's disease-related network expression with ECD SPECT. Eur J Nucl Med Mol Imaging. 2007;34(4):496–501.
156. Lin TP, et al. Metabolic correlates of subthalamic nucleus activity in Parkinson's disease. Brain. 2008;131(Pt 5):1373–80.
157. Berti V, et al. Brain metabolic correlates of dopaminergic degeneration in de novo idiopathic Parkinson's disease. Eur J Nucl Med Mol Imaging. 2010;37(3):537–44.
158. Polito C, et al. Interaction of caudate dopamine depletion and brain metabolic changes with cognitive dysfunction in early Parkinson's disease. Neurobiol Aging. 2012;33(1):206.e29–39.
159. Eidelberg D, et al. The metabolic topography of Parkinsonism. J Cereb Blood Flow Metab. 1994;14(5):783–801.
160. Eidelberg D, et al. Assessment of disease severity in Parkinsonism with fluorine-18-fluorodeoxyglucose and PET. J Nucl Med. 1995;36(3):378–83.
161. Feigin A, et al. Metabolic correlates of levodopa response in Parkinson's disease. Neurology. 2001;57(11):2083–8.
162. Lozza C, et al. Executive processes in Parkinson's disease: FDG-PET and network analysis. Hum Brain Mapp. 2004;22(3):236–45.
163. Pourfar M, et al. Assessing the microlesion effect of subthalamic deep brain stimulation surgery with FDG PET. J Neurosurg. 2009;110(6):1278–82.
164. Jourdain VA, et al. Flow-metabolism dissociation in the pathogenesis of levodopa-induced dyskinesia. JCI Insight. 2016;1(15):e86615.
165. Ko JH, et al. Network modulation following sham surgery in Parkinson's disease. J Clin Invest. 2014;124(8):3656–66.
166. Iranzo A, Santamaria J, Tolosa E. Idiopathic rapid eye movement sleep behaviour disorder: diagnosis, management, and the need for neuroprotective interventions. Lancet Neurol. 2016;15(4):405–19.
167. Ge J, et al. Assessing cerebral glucose metabolism in patients with idiopathic rapid eye movement sleep behavior disorder. J Cereb Blood Flow Metab. 2015;35(11):1902.
168. Holtbernd F, et al. Abnormal metabolic network activity in REM sleep behavior disorder. Neurology. 2014;82(7):620–7.
169. Wu P, et al. Consistent abnormalities in metabolic network activity in idiopathic rapid eye movement sleep behaviour disorder. Brain. 2014;137(Pt 12):3122–8.
170. Meles SK, et al. FDG PET, dopamine transporter SPECT, and olfaction: combining biomarkers in REM sleep behavior disorder. Mov Disord. 2017;32(10):1482–6.
171. Meles SK, et al. The metabolic pattern of idiopathic REM sleep behavior disorder reflects early-stage Parkinson's disease. J Nucl Med. 2018;59(9):1437–44.
172. Zaidel A, et al. Akineto-rigid vs. tremor syndromes in Parkinsonism. Curr Opin Neurol. 2009;22(4):387–93.
173. Antonini A, et al. The metabolic anatomy of tremor in Parkinson's disease. Neurology. 1998;51(3):803–10.

174. Feigin A, et al. Tc-99m ethylene cysteinate dimer SPECT in the differential diagnosis of Parkinsonism. Mov Disord. 2002;17(6):1265–70.
175. Habeck C, et al. A new approach to spatial covariance modeling of functional brain imaging data: ordinal trend analysis. Neural Comput. 2005;17(7):1602–45.
176. Mure H, et al. Parkinson's disease tremor-related metabolic network: characterization, progression, and treatment effects. NeuroImage. 2011;54(2):1244–53.
177. Bostan AC, Dum RP, Strick PL. The basal ganglia communicate with the cerebellum. Proc Natl Acad Sci U S A. 2010;107(18):8452–6.
178. Hoshi E, et al. The cerebellum communicates with the basal ganglia. Nat Neurosci. 2005;8(11):1491–3.
179. Lang AE. A critical appraisal of the premotor symptoms of Parkinson's disease: potential usefulness in early diagnosis and design of neuroprotective trials. Mov Disord. 2011;26(5):775–83.
180. Aarsland D, et al. Cognitive decline in Parkinson disease. Nat Rev Neurol. 2017;13(4):217–31.
181. Bohnen NI, et al. Cognitive correlates of cortical cholinergic denervation in Parkinson's disease and Parkinsonian dementia. J Neurol. 2006;253(2):242–7.
182. Emre M, et al. Rivastigmine for dementia associated with Parkinson's disease. N Engl J Med. 2004;351(24):2509–18.
183. Gratwicke J, Jahanshahi M, Foltynie T. Parkinson's disease dementia: a neural networks perspective. Brain. 2015;138(Pt 6):1454–76.
184. Kehagia AA, Barker RA, Robbins TW. Cognitive impairment in Parkinson's disease: the dual syndrome hypothesis. Neurodegener Dis. 2013;11(2):79–92.
185. Schapira AHV, Chaudhuri KR, Jenner P. Non-motor features of Parkinson disease. Nat Rev Neurosci. 2017;18(7):435–50.
186. Hosokai Y, et al. Distinct patterns of regional cerebral glucose metabolism in Parkinson's disease with and without mild cognitive impairment. Mov Disord. 2009;24(6):854–62.
187. Pappata S, et al. Mild cognitive impairment in drug-naive patients with PD is associated with cerebral hypometabolism. Neurology. 2011;77(14):1357–62.
188. Carbon M, et al. Learning networks in health and Parkinson's disease: reproducibility and treatment effects. Hum Brain Mapp. 2003;19(3):197–211.
189. Huang C, et al. Neuroimaging markers of motor and nonmotor features of Parkinson's disease: an 18f fluorodeoxyglucose positron emission computed tomography study. Dement Geriatr Cogn Disord. 2013;35(3-4):183–96.
190. Mentis MJ, et al. Relationships among the metabolic patterns that correlate with mnemonic, visuospatial, and mood symptoms in Parkinson's disease. Am J Psychiatry. 2002;159(5):746–54.
191. Huang C, et al. Metabolic abnormalities associated with mild cognitive impairment in Parkinson disease. Neurology. 2008;70(16 Pt 2):1470–7.
192. Mattis PJ, et al. Network correlates of the cognitive response to levodopa in Parkinson disease. Neurology. 2011;77(9):858–65.
193. Meles SK, et al. Abnormal metabolic pattern associated with cognitive impairment in Parkinson's disease: a validation study. J Cereb Blood Flow Metab. 2015;35(9):1478–84.
194. Mattis PJ, et al. Distinct brain networks underlie cognitive dysfunction in Parkinson and Alzheimer diseases. Neurology. 2016;87(18):1925–33.
195. Teune LK, et al. The Alzheimer's disease-related glucose metabolic brain pattern. Curr Alzheimer Res. 2014;11(8):725–32.
196. Niethammer M, et al. Parkinson's disease cognitive network correlates with caudate dopamine. NeuroImage. 2013;78:204–9.
197. Ma Y, et al. Parkinson's disease spatial covariance pattern: noninvasive quantification with perfusion MRI. J Cereb Blood Flow Metab. 2010;30(3):505–9.
198. Melzer TR, et al. Arterial spin labelling reveals an abnormal cerebral perfusion pattern in Parkinson's disease. Brain. 2011;134(Pt 3):845–55.
199. Szewczyk-Krolikowski K, et al. Functional connectivity in the basal ganglia network differentiates PD patients from controls. Neurology. 2014;83(3):208–14.
200. Wu T, et al. Functional connectivity of cortical motor areas in the resting state in Parkinson's disease. Hum Brain Mapp. 2011;32(9):1443–57.
201. Helmich RC, et al. Pallidal dysfunction drives a cerebellothalamic circuit into Parkinson tremor. Ann Neurol. 2011;69(2):269–81.
202. Wu T, et al. Parkinson's disease-related spatial covariance pattern identified with resting-state functional MRI. J Cereb Blood Flow Metab. 2015;35(11):1764–70.
203. Beckmann CF, et al. Investigations into resting-state connectivity using independent component analysis. Philos Trans R Soc Lond Ser B Biol Sci. 2005;360(1457):1001–13.
204. Calhoun VD, Liu J, Adali T. A review of group ICA for fMRI data and ICA for joint inference of imaging, genetic, and ERP data. NeuroImage. 2009;45(1 Suppl):S163–72.
205. Vo A, et al. Parkinson's disease-related network topographies characterized with resting state functional MRI. Hum Brain Mapp. 2017;38(2):617–30.
206. Sporns O. Contributions and challenges for network models in cognitive neuroscience. Nat Neurosci. 2014;17(5):652–60.
207. Correa CD, Crnovrsanin T, Ma KL. Visual reasoning about social networks using centrality sensitivity. IEEE Trans Vis Comput Graph. 2012;18(1):106–20.
208. Bassett DS, Bullmore ET. Small-world brain networks revisited. Neuroscientist. 2016;23(5):499–516.
209. Helmich RC. The cerebral basis of Parkinsonian tremor: a network perspective. Mov Disord. 2018;33(2):219–31.
210. Ma H, et al. Resting-state functional connectivity of dentate nucleus is associated with tremor in Parkinson's disease. J Neurol. 2015;262(10):2247–56.
211. Ma LY, et al. Disrupted brain network hubs in subtype-specific Parkinson's disease. Eur Neurol. 2017;78(3-4):200–9.
212. Baggio HC, et al. Functional brain networks and cognitive deficits in Parkinson's disease. Hum Brain Mapp. 2014;35(9):4620–34.
213. Pereira JB, et al. Aberrant cerebral network topology and mild cognitive impairment in early Parkinson's disease. Hum Brain Mapp. 2015;36(8):2980–95.
214. Hellwig S, et al. [(1)(8)F]FDG-PET is superior to [(1)(2)(3)I] IBZM-SPECT for the differential diagnosis of Parkinsonism. Neurology. 2012;79(13):1314–22.
215. Ge J, et al. Reproducible network and regional topographies of abnormal glucose metabolism associated with progressive supranuclear palsy: multivariate and univariate analyses in American and Chinese patient cohorts. Hum Brain Mapp. 2018;39(7):2842–58.
216. Niethammer M, et al. A disease-specific metabolic brain network associated with corticobasal degeneration. Brain. 2014;137(Pt 11):3036–46.
217. Spetsieris P, et al. Differential diagnosis of Parkinsonian syndromes using PCA-based functional imaging features. NeuroImage. 2009;45(4):1241–52.
218. Holtbernd F, Eidelberg D. The utility of neuroimaging in the differential diagnosis of Parkinsonian syndromes. Semin Neurol. 2014;34(2):202–9.
219. Tang CC, et al. Differential diagnosis of Parkinsonism: a metabolic imaging study using pattern analysis. Lancet Neurol. 2010;9(2):149–58.
220. Tripathi M, et al. Metabolic image-based algorithm for accurate differential diagnosis of Parkinsonism: prospective validation in Indian patient population. J Nucl Med. 2012;53(Suppl 1):1974.

221. Boeve BF. The multiple phenotypes of corticobasal syndrome and corticobasal degeneration: implications for further study. J Mol Neurosci. 2011;45(3):350–3.
222. Hassan A, Whitwell JL, Josephs KA. The corticobasal syndrome-Alzheimer's disease conundrum. Expert Rev Neurother. 2011;11(11):1569–78.
223. Hu WT, et al. Alzheimer's disease and corticobasal degeneration presenting as corticobasal syndrome. Mov Disord. 2009;24(9):1375–9.
224. Litvan I, et al. Accuracy of the clinical diagnosis of corticobasal degeneration: a clinicopathologic study. Neurology. 1997;48(1):119–25.
225. Garraux G, et al. Multiclass classification of FDG PET scans for the distinction between Parkinson's disease and atypical Parkinsonian syndromes. Neuroimage Clin. 2013;2:883–93.
226. Mudali D, et al. Classification of Parkinsonian syndromes from FDG-PET brain data using decision trees with SSM/PCA features. Comput Math Methods Med. 2015;2015:136921.
227. Schwingenschuh P, et al. Distinguishing SWEDDs patients with asymmetric resting tremor from Parkinson's disease: a clinical and electrophysiological study. Mov Disord. 2010;25(5):560–9.
228. LeWitt PA, et al. AAV2-GAD gene therapy for advanced Parkinson's disease: a double-blind, sham-surgery controlled, randomised trial. Lancet Neurol. 2011;10(4):309–19.
229. Niethammer M, et al. Long-term follow-up of a randomized AAV2-GAD gene therapy trial for Parkinson's disease. JCI Insight. 2017;2(7):e90133.
230. Niethammer M, et al. Gene therapy reduces Parkinson's disease symptoms by reorganizing functional brain connectivity. Sci Transl Med. 2018;10(469):aau0713.
231. Galpern WR, et al. Sham neurosurgical procedures in clinical trials for neurodegenerative diseases: scientific and ethical considerations. Lancet Neurol. 2012;11(7):643–50.
232. Espay AJ, et al. Placebo effect of medication cost in Parkinson disease: a randomized double-blind study. Neurology. 2015;84(8):794–802.
233. Guttman M, et al. Brain serotonin transporter binding in non-depressed patients with Parkinson's disease. Eur J Neurol. 2007;14(5):523–8.
234. Kerenyi L, et al. Positron emission tomography of striatal serotonin transporters in Parkinson disease. Arch Neurol. 2003;60(9):1223–9.
235. Politis M, et al. Staging of serotonergic dysfunction in Parkinson's disease: an in vivo 11C-DASB PET study. Neurobiol Dis. 2010;40(1):216–21.
236. Albin RL, et al. Spared caudal brainstem SERT binding in early Parkinson's disease. Journal of Cereb Blood Flow Metab. 2008;28(3):441–4.
237. Politis M, et al. Depressive symptoms in PD correlate with higher 5-HTT binding in raphe and limbic structures. Neurology. 2010;75(21):1920–7.
238. Maillet A, et al. The prominent role of serotonergic degeneration in apathy, anxiety and depression in de novo Parkinson's disease. Brain. 2016;139(Pt 9):2486–502.
239. Wilson H, et al. Serotonergic dysregulation is linked to sleep problems in Parkinson's disease. Neuroimage Clin. 2018;18:630–7.
240. Doder M, et al. Tremor in Parkinson's disease and serotonergic dysfunction: an 11C-WAY 100635 PET study. Neurology. 2003;60(4):601–5.
241. Politis M, et al. Serotonergic neurons mediate dyskinesia side effects in Parkinson's patients with neural transplants. Science Transl Med. 2010;2(38):38ra46.
242. Politis M, et al. Serotonergic mechanisms responsible for levodopa-induced dyskinesias in Parkinson's disease patients. J Clin Invest. 2014;124(3):1340–9.
243. Carta M, Bjorklund A. The serotonergic system in L-DOPA-induced dyskinesia: pre-clinical evidence and clinical perspective. J Neural Transm. 2018;125(8):1195–202.
244. Roselli F, et al. Midbrain SERT in degenerative Parkinsonisms: a 123I-FP-CIT SPECT study. Mov Disord. 2010;25(12):1853–9.
245. Koch W, et al. Extrastriatal binding of [(1)(2)(3)I]FP-CIT in the thalamus and pons: gender and age dependencies assessed in a European multicentre database of healthy controls. Eur J Nucl Med Mol Imaging. 2014;41(10):1938–46.
246. Joling M, et al. Striatal DAT and extrastriatal SERT binding in early-stage Parkinson's disease and dementia with Lewy bodies, compared with healthy controls: an (123)I-FP-CIT SPECT study. Neuroimage Clin. 2019;22:101755.
247. Pilotto A, et al. Extrastriatal dopaminergic and serotonergic pathways in Parkinson's disease and in dementia with Lewy bodies: a (123)I-FP-CIT SPECT study. Eur J Nucl Med Mol Imaging. 2019;46(8):1642–51.
248. Fazio P, et al. High-resolution PET imaging reveals subtle impairment of the serotonin transporter in an early non-depressed Parkinson's disease cohort. Eur J Nucl Med Mol Imaging. 2020;47(10):2407–16.
249. Imamura K, et al. Cytokine production of activated microglia and decrease in neurotrophic factors of neurons in the hippocampus of Lewy body disease brains. Acta Neuropathol. 2005;109(2):141–50.
250. Imamura K, et al. Distribution of major histocompatibility complex class II-positive microglia and cytokine profile of Parkinson's disease brains. Acta Neuropathol. 2003;106(6):518–26.
251. Ishizawa K, Dickson DW. Microglial activation parallels system degeneration in progressive supranuclear palsy and corticobasal degeneration. J Neuropathol Exp Neurol. 2001;60(6):647–57.
252. Ishizawa K, et al. Microglial activation parallels system degeneration in multiple system atrophy. J Neuropathol Exp Neurol. 2004;63(1):43–52.
253. Papadopoulos V, et al. Translocator protein (18kDa): new nomenclature for the peripheral-type benzodiazepine receptor based on its structure and molecular function. Trends Pharmacol Sci. 2006;27(8):402–9.
254. Varnas K, et al. PET imaging of [(11)C]PBR28 in Parkinson's disease patients does not indicate increased binding to TSPO despite reduced dopamine transporter binding. Eur J Nucl Med Mol Imaging. 2019;46(2):367–75.
255. Venneti S, Lopresti BJ, Wiley CA. The peripheral benzodiazepine receptor (translocator protein 18kDa) in microglia: from pathology to imaging. Prog Neurobiol. 2006;80(6):308–22.
256. Cicchetti F, et al. Neuroinflammation of the nigrostriatal pathway during progressive 6-OHDA dopamine degeneration in rats monitored by immunohistochemistry and PET imaging. Eur J Neurosci. 2002;15(6):991–8.
257. Real CC, et al. Evaluation of exercise-induced modulation of glial activation and dopaminergic damage in a rat model of Parkinson's disease using [(11)C]PBR28 and [(18)F]FDOPA PET. J Cereb Blood Flow Metab. 2019;39(6):989–1004.
258. Gerhard A, et al. In vivo imaging of microglial activation with [11C](R)-PK11195 PET in idiopathic Parkinson's disease. Neurobiol Dis. 2006;21(2):404–12.
259. Ouchi Y, et al. Microglial activation and dopamine terminal loss in early Parkinson's disease. Ann Neurol. 2005;57(2):168–75.

260. Ouchi Y, et al. Neuroinflammation in the living brain of Parkinson's disease. Parkinsonism Relat Disord. 2009;15(Suppl 3):S200–4.
261. Edison P, et al. Microglia, amyloid, and glucose metabolism in Parkinson's disease with and without dementia. Neuropsychopharmacology. 2013;38(6):938–49.
262. Fan Z, et al. Influence of microglial activation on neuronal function in Alzheimer's and Parkinson's disease dementia. Alzheimers Dement. 2015;11(6):608–21. e7
263. Bartels AL, Leenders KL. Neuroinflammation in the pathophysiology of Parkinson's disease: evidence from animal models to human in vivo studies with [11C]-PK11195 PET. Mov Disord. 2007;22(13):1852–6.
264. Bartels AL, et al. [11C]-PK11195 PET: quantification of neuroinflammation and a monitor of anti-inflammatory treatment in Parkinson's disease? Parkinsonism Relat Disord. 2010;16(1):57–9.
265. Ghadery C, et al. Microglial activation in Parkinson's disease using [(18)F]-FEPPA. J Neuroinflammation. 2017;14(1):8.
266. Koshimori Y, et al. Imaging striatal microglial activation in patients with Parkinson's disease. PLoS One. 2015;10(9):e0138721.
267. Mizrahi R, et al. Translocator protein (18 kDa) polymorphism (rs6971) explains in-vivo brain binding affinity of the PET radioligand [(18)F]-FEPPA. J Cereb Blood Flow Metab. 2012;32(6):968–72.
268. Owen DR, et al. An 18-kDa translocator protein (TSPO) polymorphism explains differences in binding affinity of the PET radioligand PBR28. J Cereb Blood Flow Metab. 2012;32(1):1–5.